

RESEARCH ARTICLE

Targeting of Photoreceptor Genes in *Chlamydomonas reinhardtii* via Zinc-finger Nucleases and CRISPR/Cas9

Andre Greiner^{a1, 2}, Simon Kelterborn^{a1}, Heide Evers^a, Georg Kreimer^b, Irina Sizova^{a2, 3}, and Peter Hegemann^a

^aInstitute of Biology, Experimental Biophysics, Humboldt-Universität zu Berlin, Berlin, Germany

^bDepartment of Biology, Friedrich-Alexander-University, 91058 Erlangen, Germany

¹These authors contributed equally to this research

²Corresponding Authors: irinasiz@yahoo.com and andregrein@gmail.com

³Permanent address: Division of Radiation Biophysics, Petersburg Nuclear Physics Institute, Russian Academy of Sciences, Gatchina/St. Petersburg, 188350, Russia

Short title: *Chlamydomonas* gene editing

One-sentence summary: Using optimized protocols, nuclear photoreceptor genes were successfully modified or inactivated in the alga *Chlamydomonas* via directed gene targeting using zinc finger nucleases or the nuclease Cas9.

The authors responsible for distribution of materials integral to the findings presented in this article in accordance with the policy described in the Instructions for Authors (www.plantcell.org) are: Irina Sizova (irinasiz@yahoo.com) and Andre Greiner (andregrein@gmail.com).

ABSTRACT

The fast-growing biflagellated single celled chlorophyte *Chlamydomonas reinhardtii* is the most widely used alga in basic research. The physiological functions of the 18 sensory photoreceptors are of particular interest with respect to *C. reinhardtii* development and behavior. Despite the demonstration of gene editing in *C. reinhardtii* in 1995, the isolation of mutants lacking easily ascertained newly acquired phenotypes remains problematic due to low DNA recombination efficiency. We **optimized** gene-editing protocols for several *Chlamydomonas* strains (including wild-type CC-125) using **zinc-finger nucleases (ZFNs)**, genetically encoded CRISPR/associated protein 9 (Cas9) from *Staphylococcus aureus* and *Streptococcus pyogenes*, and recombinant Cas9 and developed protocols for rapidly isolating non-selectable gene mutants. Using this technique, we disrupted the photoreceptor genes *COP1/2*, *COP3* (encoding channelrhodopsin-1 [ChR1]), *COP4* (encoding ChR2), *COP5*, ***PHOT***, *UVR8*, *VGCC*, *MAT3* and *aCRY* and created the *chr1*, *chr2* and *uvr8* *phot* double mutants. Characterization of the *chr1*, *chr2* and *mat3* mutants confirmed the value of photoreceptor mutants for physiological studies. Genes of interest were disrupted in 5–15% of preselected clones (~1 out of 4000 initial cells). Using ZFNs, genes were edited in a reliable, predictable manner via homologous recombination, whereas Cas9 primarily caused gene disruption via the insertion of co-transformed DNA. These methods should be widely applicable to research involving green algae.

1 INTRODUCTION

2 Light provides both energy and information to guide or affect plant and algal growth,
3 development, orientation, adaptation, and stress responses. Whereas energy conversion via
4 photosynthesis is widely understood, our knowledge of the signaling processes initiated by light
5 through sensory photoreceptors remains fragmentary, despite considerable research over the past
6 three decades. The fast, synchronized growth of *Chlamydomonas reinhardtii* (hereafter
7 *Chlamydomonas*), its ability to grow **heterotrophically** and the extensive knowledge of its
8 biochemistry, cellular and molecular biology that has accumulated over the past decades has
9 rendered it an excellent organism to study complex networks of sensory photoreceptors. To date,
10 18 photoreceptor genes have been assigned in the *Chlamydomonas* genome (Figure 1). Some of
11 these genes are more or less universal, such as *UVR8*, which encodes a homomultimeric UV-B
12 photoreceptor that monomerizes upon UV-B reception to regulate gene expression (e.g., in UV-B
13 acclimation and stress responses). However, the specific physiological functions are largely
14 unknown for the light-sensitive cryptochrome proteins, of which *Chlamydomonas* contains four
15 variants: aCRY, pCRY, CRY-DASH-1, and CRY-DASH-2 (Spexard et al. 2014; Beel et al.
16 2012). Nevertheless, there is evidence that aCRY modulates the expression of several genes in
17 response to blue, orange, and red light. The unique red-light response of aCRY has been linked to
18 the neutral radical of the flavin chromophore acting as a sensor that absorbs light over almost the
19 entire visible spectral range up to 680 nm (Spexard et al. 2014; Beel et al. 2012). Additionally,
20 recent evidence points to a central role for pCRY in controlling the circadian clock and the algal
21 life cycle (Muller et al. 2017) and to an involvement of CRY in the sexual life cycle (Zou et al.
22 2017).

23 Although *Chlamydomonas reinhardtii* is widely used in basic and applied research and
24 important discoveries including sensory photoreceptors have been made using this organism,
25 functional studies involving *Chlamydomonas* have been limited by difficulties in modifying or
26 inactivating genes by directed gene targeting. Homologous recombination (HR) between
27 endogenous DNA and homologous DNA templates in *C. reinhardtii* is rare because double-strand
28 breaks (DSBs)—if they occur—are in most cases repaired via error prone non-homologous end
29 joining (NHEJ) rather than high-fidelity homology-directed repair (HDR) (Zorin et al. 2005), thus
30 impeding targeted gene modification. More recently, several attempts were made to improve the
31 HDR frequency and suppress NHEJ in *Chlamydomonas*. A single-stranded DNA (ssDNA)

approach enabling marked suppression of random integration of template DNA allowed for the inactivation of the phototropin-encoding *PHOT* gene in the non-motile *C. reinhardtii* strain CW15-302 (also named CC-4350) with an efficiency of ~1% in co-selected mutants (Zorin et al. 2009). The disruption of *PHOT* suppressed both **eyespot size reduction** and downregulation of channelrhodopsin at high light intensities (Trippens et al. 2012), as well as high-energy non-photochemical quenching, which dissipates harmful excessive light energy in photosystem II as heat to prevent protein damage (Petroutsos et al. 2016).

Further advances in developing techniques for increasing the frequency of HDR in *C. reinhardtii* were realized by exploiting zinc-finger nuclease (ZFN) technology (Bibikova et al. 2003), which produces targeted DNA-DSBs suitable for the insertion of templates via HDR. *COP3*, which encodes channelrhodopsin-1 (ChR1), was inactivated by HDR using the ZFN approach (Sizova et al. 2013). ChR1 and ChR2 are the most well-characterized sensory photoreceptors in *C. reinhardtii* to date (Schneider et al. 2015; Deisseroth and Hegemann 2017). The inactivation of *COP3* and *COP4* (which encodes ChR2) using antisense approaches revealed that both proteins are photoreceptors for phototactic and photophobic responses via previously described photocurrents (Harz et al. 1992; Holland et al. 1996; Braun and Hegemann 1999; Sineshchekov et al. 2002; Govorunova et al. 2004; Berthold et al. 2008). Electrical studies in ChR1 and ChR2 expressing *Xenopus* oocytes and HEK (human embryonic kidney) cells revealed that both proteins function as light-gated ion channels (Nagel et al. 2002; Nagel et al. 2003). More detailed physiologic studies of ChR function and processing would require disruption of the genes encoding both ChR1 and ChR2 and replacement with genes encoding modified ChR variants. Moreover, neither of the above-described earlier approaches (ssDNA- or ZFN-based) enabled a gene of interest (GOI) to be targeted in motile *C. reinhardtii* strains (Sizova et al. 2013).

Although the ZFN-technology has proven to be useful in single knock-out experiments and for promoting HDR, this technology was likely too limited to be used to investigate the four cryptochrome and eight enzyme rhodopsin photoreceptors (Figure 1) with strong sequence homology and (probably) functions. The latter family, named histidinkinase rhodopsins (HKR1-HKR8, encoded by the genes *COP5–COP12*) is characterized by the presence of microbial-type sensory rhodopsins connected C-terminally to a histidine kinase and a response regulator (Kateriya et al. 2004). HKR1, 2, and 4–6 contain a C-terminal guanylyl- or adenylyl-cyclase effector domain, suggesting that HKRs regulate cGMP and cAMP (Figure 1). Little is known

63 about the HKRs aside from data regarding the photophysics and photochemistry of the bimodally
64 switchable HKR1 photoreceptor (Luck et al. 2012; Penzkofer et al. 2014; Luck and Hegemann
65 2017).

66 By far the most popular and widely used programmable nuclease system for gene
67 modification in many organisms is clustered regularly interspaced short palindromic repeat
68 (CRISPR)/associated protein 9 (Cas9) technology (Jinek et al. 2012; Mali et al. 2013; Jinek et al.
69 2013; Cong et al. 2013). The CRISPR DNA-targeting system consists of three components: Cas9
70 nuclease protein; complementary base-pairing CRISPR RNA (crRNA), which includes the target
71 sequence (protospacer); and trans-activating CRISPR RNA (tracrRNA), which forms a secondary
72 scaffold structure recognized by Cas9. By inserting a small linker sequence, the crRNA:tracrRNA
73 duplex can be expressed as a single guide RNA (sgRNA) that binds to the Cas9 nuclease to form
74 a Cas9/sgRNA ribonucleoprotein (RNP) complex. The only prerequisite for target DNA
75 recognition by the Cas9 RNP is the protospacer adjacent motif (PAM), which varies among Cas9
76 variants and is located immediately downstream of the target sequence. In the first Cas9
77 discovered, SpCas9 (from *Streptococcus pyogenes*), the PAM motif is NGG, whereas in Cas9
78 from *Staphylococcus aureus* (SaCas9), the PAM motif is NNGRRT, where R indicates either
79 adenine or guanine.

80 Three research groups have reported using the CRISPR/Cas9 system in *C. reinhardtii*
81 (Jiang et al. 2013; Baek et al. 2016; Shin et al. 2016; Jiang et al. 2014; Jiang and Weeks 2017).
82 Promising results were achieved when Cas9/sgRNA RNP complexes assembled *in vitro* were
83 delivered into *Chlamydomonas* cells via electroporation (Baek et al. 2016; Shin et al. 2016). After
84 targeting the photosynthesis-associated genes *ZEP*, *CpFTSY*, *CpSRP43*, and *ChLM*, some of the
85 colonies (which were preselected with an antibiotic resistance marker) appeared pale due to
86 reduced antenna size and/or chlorophyll synthesis (Kirst et al. 2012; Meinecke et al. 2010). The
87 targeting efficiency (targeted colonies/selected colonies) obtained from visual clone identification
88 in these studies was approximately 1:600 (0.17%), 1:73 (1.4%) (Shin et al. 2016), and 0.56%
89 (Baek et al. 2016). Earlier, another group established a plasmid-based CRISPR/Cas9 system in
90 *Chlamydomonas* (Jiang et al. 2014). In their initial approach, the authors targeted the peptidyl-
91 prolyl *cis-trans* isomerase gene *FKB12*, allowing for positive selection of cells with *FKB12* gene
92 knockouts on medium containing rapamycin. This resulted in the production of one mutant
93 colony out of 16 transformations, or 1 colony with a modified target locus per 1.5×10^9 initial

94 cells (Jiang et al. 2014). Later, using a hybrid Cas9/sgRNA expression construct, the efficiency
95 was improved to yield 13 colonies out of 4 transformations (equivalent to ~1 colony per 3×10^7
96 initial cells) (Jiang and Weeks 2017). Additionally, positive selection of prototrophic strains after
97 precise repair of the point mutation in the *ARG* gene in the auxotrophic mutant, *arg7*, was
98 demonstrated using the hybrid Cas9/sgRNA gene co-electroporated with a short, 80 nucleotide,
99 ssODN (oligodeoxynucleotide) with 5' and 3' phosphothioate (PTO)-protected ends. In this study,
100 7 arginine prototroph clones were isolated from 2 transformation reactions (~1 colony per 2.5×10^7
101 initial cells) (Jiang and Weeks 2017). These results indicate that the CRISPR/Cas9 system is
102 suitable for gene modification in *C. reinhardtii*. However, the efficiency of the reported methods
103 is low, and the methods do not enable routine disruption of non-selectable or non-phenotypic
104 genes.

105 Our goal in the present study was to overcome the drawbacks associated with existing
106 methods and to optimize gene targeting in *Chlamydomonas* by developing a technology that (i)
107 allows for efficient gene disruption and ultimately precise and predictable gene editing via HR;
108 (ii) enables efficient isolation of non-phenotypic mutants; and (iii) is applicable to numerous
109 *Chlamydomonas* strains. Towards this end, we optimized ZFN technology to enable precise gene
110 modification in *Chlamydomonas*. We then modified these protocols further for CRISPR/Cas9 to
111 disrupt genes rapidly and in a cost-effective, routine manner.

112

113 RESULTS

114 A selectable marker repair assay to evaluate target-specific zinc-finger nucleases

115 To elucidate the roles of *ChR1* and *ChR2* in phototactic and photophobic responses in detail,
116 single and double *ChR1* and *ChR2* knockouts are required. We previously reported the
117 development and application of *ChR1*-specific ZFNs in the non-motile *C. reinhardtii* strain
118 CW15-302 (Sizova et al. 2013). In a continuation of this work, we utilized these nucleases in a
119 motile *Chlamydomonas* strain to develop *ChR2*-specific ZFNs. We analyzed *ChR2* for ZFN target
120 sites using the ZiFiT (Zinc Finger Targeter) database (Sander et al. 2007). As predictions gave
121 rise to only a poorly active *ChR2*-ZFN pair (hereafter designated ChR2-a-ZFNs), we ordered a set
122 of *ChR2*-ZFNs from a commercial supplier (hereafter designated ChR2-b-ZFNs). To characterize
123 both nuclease pairs, we used an optimized version (Figure 2A) of the previously reported mutated

124 *aphVIII* (mut-*aphVIII*) repair gene targeting selection (GTS) system (Sizova et al. 2013)
125 (explained in detail below) to qualify HDR of nuclear genes in *C. reinhardtii*.

126 The GTS construct (*ble:yfp:mut-aphVIII*; Figure 2A and Supplemental Table 1) for
127 creating the GTS test strains was improved by replacing rarely used (<15%) codons at the 5' end
128 of the *ble* (phleomycin [Zeocin™]-resistance gene [ZcR]), substituting the previously used *gfp*
129 gene (Fuhrmann et al. 1999) with the codon-optimized enhanced *yfp* gene (*eyfp*), and inserting a
130 glycine-serine linker between *eyfp* and the mutated *aphVIII* selection marker. The linker was
131 inserted to separate the *ble* and *eyfp* protein domains to potentially preserve their activities and
132 stabilize the fusion protein by preventing premature protein degradation. The *aphVIII*
133 (paromomycin resistance, PmR) gene was mutated by inserting target sites for the previously
134 functionally characterized ChR1-ZFNs (Sizova et al. 2013) and the newly designed but
135 uncharacterized ChR2-a-ZFNs (pGTS1-mut-*aphVIII*^{[ChR2-a][ChR1]}; Figure 2A). Cell wall-deficient,
136 motile *C. reinhardtii* strain CC-3403 (RU-387 nit1 arg7 cw15 mt-) cells were transfected with
137 pGTS1 via electroporation. Full-length integration of the GTS1 cassette was confirmed by PCR
138 analysis of genomic DNA isolated from ZcR clones. The verified clonal cell line was designated
139 the “GTS-strain.” After a second round of electroporation of the GTS-strain with ZFN-encoding
140 plasmids (Figure 2C), functional ZFNs recognized and cleaved their respective mut-*aphVIII*
141 target sites. The resulting DNA-DSBs triggered the cellular DNA repair machinery to utilize a co-
142 supplied repair-donor to restore *aphVIII* functionality (Figure 2C), thereby creating selectable
143 PmR clones. The number of PmR clones served as an indicator of nuclease functionality. The
144 GTS approach thus allows for testing and optimization of many parameters that could limit HDR-
145 based modification of *Chlamydomonas* genes, such as nuclease activity, HDR-donor design, and
146 transformation conditions.

147 **Highly active *FokI* enables HDR of endogenous genes in strains CC-3403 and CC-503**

148 The objective of our first experiments was to test the overall functionality of the GTS system in
149 the CC-3403 background. Verified 3403-GTS1 (pGTS1 in CC-3403) cells were grown
150 synchronously before electroporation of ChR1-ZFN plasmids and mut-*aphVIII* repair templates
151 (pHDR-APHVIII^{Δ120}; Figure 2A and C). Employment of the heat-shock protein (HSP) 70A
152 promoter (triggered by a short heat shock of 30 min at 40°C before electroporation) was expected

153 to allow for time-limited ZFN transcription and to minimize possible toxic effects resulting from
154 long-term nuclease expression (Schroda et al. 2000) Sizova et al. 2013).

155 ZFNs are artificial restriction enzymes consisting of 3–4 zinc-finger DNA binding
156 modules fused to the heterodimeric nuclease domain *FokI* (Miller et al. 2007). Using strain 3403-
157 GTS1, we tested two different engineered *FokI* heterodimer variants (Guo et al. 2010; Sizova et
158 al. 2013) in combination with ChR1-ZFNs. *FokI* variant S418R/K441E, originally optimized for
159 CW15-302 cells (Sizova et al. 2013), generated only a limited number of PmR colonies after
160 electroporation and selection, similar to the control. The more active *FokI* variant *FokI*-
161 S418P/K441E (SP/KE) was more efficient with respect to mut-*aphVIII* repair, generating ~500
162 colonies per electroporation (Figure 2D). For comparison, glass-bead transformation (Kindle
163 1990) with ChR1-ZFNs (*FokI*-SP/KE) resulted in only 6±2 PmR colonies. Thus, we used *FokI*-
164 KE/SP and electroporation in subsequent ZFN experiments.

165 We then tested the two new pairs of ChR2-ZFNs. Using ChR2-a-ZFNs (with *FokI*-SP/KE)
166 in strain 3403-GTS1, very few (n=15) PmR colonies appeared. By contrast, ChR2-b-ZFNs were
167 50% more active than the ChR1-ZFNs in strain 3403-GTS2 with both ChR1 and ChR2-b target
168 sites included (mut-*aphVIII* [^{[ChR2-b][ChR1]}]) (Figure 2D). Similar repair efficiencies were observed
169 for 503-GTS2 cells derived from strain CC-503 (Figure 2D). We concluded that the previously
170 reported high level of transgene expression in CW15-302 is disadvantageous in combination with
171 the use of highly active *FokI*-SP/KE ZFNs. The superior performance of the more active ZFN
172 variants in CC-3403 and CC-503 cells compared with CW15-302 cells is thus most likely
173 associated with lower levels of transgene expression (Sizova et al. 2013).

174

175 **Short HDR donors enhance mutant screening efficiency**

176 To simplify donor generation and analysis of potential *ChR1* and *ChR2* (or any GOI)
177 recombinants, we tested shorter templates in the mut-*aphVIII* repair assay. We compared circular
178 plasmids (1350 bp), short double-stranded linear fragments with 5'-phosphorothioate (PTO)-
179 blocking groups (500 bp), and single-stranded oligodeoxynucleotides (ssODNs) with 5'- and 3'-
180 PTO protections (100 nt) as templates in the GTS system (Liang et al. 2017; Jiang et al. 2017). As
181 expected, a shorter template homology region was correlated with fewer PmR colonies (Figure
182 2D; dark blue bars (i) 994±65, (ii) 570±15, and (iii) 266±93), respectively, for plasmids, short
183 double-stranded linear fragments with 5'-PTO blocking groups, and ssODNs with 5'- and 3'-PTO

184 protections). However, all tested small donors promoted mut-*aphVIII* HDR at reasonable
185 frequencies. In our protocol, cells were allowed to recover for 24 h at room temperature (22°C)
186 before plating. Increasing the recovery temperature from 22 to 33°C increased the number of
187 colonies by 25 to 90%, depending on the template (Figure 2D; white bars (i) 1238±190, (ii)
188 709±427, and (iii) 508±130). For each donor type, we sequenced four PmR clones. With the
189 ssODN template, only one PmR clone contained an integrated silent, single point mutation,
190 whereas the 11 other sequenced clones carried repaired *aphVIII*, as specified by the template
191 (Figure 2E). With respect to the proportion of PmR colonies, we achieved editing efficiencies in
192 the range of 2.5×10^{-5} to 2.5×10^{-4} (1 HDR event per 4,000 cells).

193

194 **ZFN-mediated disruption of non-selectable genes for ChR1 and ChR2**

195 After these optimization experiments in GTS-strains, we next targeted the endogenous *ChR1* and
196 *ChR2* genes in strain CC-3403. Prior electrode voltage clamp studies revealed that ChR1 and
197 ChR2 directly function as light-gated ion channels (Nagel et al. 2002; Nagel et al. 2003). The
198 light sensor and channel pore is confined to the 7-transmembrane helix fragment of the proteins,
199 whereas the long C-terminus is likely responsible for membrane targeting to the eyespot
200 (Mittelmeier et al. 2011). First, we tested whether these proteins are the only photoreceptors
201 mediating phototaxis by creating protein-coding disruptive HDR knock-in templates for both
202 genes (Figure 3A-B). As CC-3403 is an arginine auxotroph and therefore requires arginine
203 supplementation in the medium, we used the argininosuccinate lyase gene *ARG7* (pHR11) as a
204 selection marker in cotransformation experiments with ZFNs and HDR donors. Correct donor
205 integration introduced an additional 30 bp to the sequence, referred to as “FLAG” in the
206 following experiments, that was utilized for unique oligodeoxynucleotide (ODN) binding in our
207 HDR-specific PCR screening strategy (Figure 3A, blue arrow). In an experiment targeting the
208 *ChR1* gene, eight out of 96 analyzed arginine prototroph clones exhibited donor integration
209 (Figure 3C). In seven *chr1* clones, the HDR donor had been correctly inserted (FLAG Insert;
210 Figure 3C-D; *chr1* [1-7]). In one clone, the donor had been integrated via 5' HR of the
211 cleavage site, but it also contained additional plasmid DNA fragments. For *ChR2*, we screened 96
212 clones each from three independent transformation experiments and found 22 “FLAG”-insertions
213 (7.6% on average, Figure 3C). Of the 16 sequenced *chr2* clones, 15 contained a correctly inserted
214 HDR donor (Figure 3D; *chr2* [1-15]) and in only one clone, the template plus parts of plasmid

215 DNA had been integrated by NHEJ at the 3' site (*chr2* [16]). In controls without an HDR donor,
216 we found two mutants out of 96 clones with small mutations at the target site (Figure 3C-D; *chr2*
217 [17+18]). To generate a strain where both ChRs are disrupted, we transformed strain 3403-*chr1-1*
218 with ChR2-ZFNs and ChR2-HDR donor and co-selected them using an *aphVIII* marker gene. In
219 six out of 96 analyzed clones, both *ChR1* and *ChR2* were disrupted (Figure 3C-D; *chr1 chr2* [1-
220 6]). Protein immunoblots using a ChR1-specific antiserum (Nagel et al. 2003) demonstrated the
221 absence of ChR1 in the *chr1-1* strains, and only very low amounts of ChR1:FLAG (Δ CT) of a
222 reduced size were detected (Figure 3E). Unfortunately, our ChR2 antiserum cross-reacted with
223 ChR1 and due to the similar molecular weights of both ChRs, ChR2 was only detectable by
224 immunoblotting protein extracts from CC-3403-*chr1* cells. In strain CC-3403-*chr1-1*, ChR2
225 comprised only a minor fraction (Figure 3F) and disappeared in the double knockout strain CC-
226 3403-*chr1-1/chr2-1* (Figure 3F). The single and double-knockout strains were motile and suitable
227 for physiological studies.

228

229 **Photomovement analysis of *ChR1* and *ChR2* disruption strains**

230 We performed light scattering (LS) assays to quantify the phototactic sensitivity of the strains
231 (Uhl and Hegemann 1990). The LS signals from CC-3403 gamete cells were nearly identical to
232 those of previously studied CW2 cells (Berthold et al. 2008). After lights-on, the LS signal
233 linearly rose until it approached a stationary level (Figure 4A). Under low intensity light (455
234 nm), the increase was graded with the light intensity over 1.5 log units. However, phototaxis was
235 delayed at higher intensities due to a transient switch from forward to reverse swimming during
236 the phobic response (Figure 4A) (Hegemann and Bruck 1989). The behavior and light sensitivity
237 in *chr2* cells were almost indistinguishable from those of the parent cells at both 455 nm and 530
238 nm wavelengths (Figure 4A-B; light blue), confirming that ChR1, with an absorption maximum
239 $\lambda_{\text{max}}=495$ nm at pH 6.5, is the dominant phototaxis photoreceptor in CC-3403 cells. In contrast,
240 *chr1* showed an almost 1000-fold lower sensitivity at 455 nm (Figure 4A-B; dark blue), where
241 ChR1 and ChR2 absorb light equally well (Berthold et al. 2008). Photoorientation was almost
242 undetectable in the *chr1 chr2* double mutant (Figure 4A-B, light grey). These results confirm that
243 while both ChRs are phototaxis photoreceptors, ChR2 has a low abundance and is only a minor
244 contributor to the phototactic sensitivity and performance of CC-3404 cells.

245

246 **Analysis of eyespots in *ChR1* and *ChR2* disruption strains**

247 As a second physiological approach, we explored the C-terminus of ChR1 and its role in the
248 transport of ChR to the eyespot. All HDR templates designed to this point contained a short insert
249 of only ~30 bp. However, we were interested in labeling algal proteins with fluorescent tags. As
250 proof of principle, we created a new donor that included the coding sequence for mCherry in-
251 frame, interspacing the ChR1-ZFN target site located on the C-terminus of the respective ChR1
252 protein (pHDR-ChR1:mCherry; Figure 3A-B). The mCherry sequence was correctly inserted and
253 expressed in ~1% of analyzed clones (3/288). Confocal microscopy confirmed ChR1-tagging
254 (Figure 4 C-D). However, only a minor fraction of the ChR1:mCherry protein was targeted to the
255 eyespot (Berthold et al. 2008; Mittelmeier et al. 2011), whereas the main fraction was localized as
256 patches within the cell (Figure 4D). Nevertheless, an eyespot was visible in the strains with an
257 mCherry-tagged ChR1.

258 Next, we analyzed whether the different ChR modified strains developed alterations in
259 eyespot positioning and size, as measured by examining the carotenoid-rich eyespot globule
260 layers visible via differential interference microscopy. All strains in non-synchronous growing
261 cultures had visible eyespots, as exemplified in the wild-type-like CC-3403, strain *chr1 chr2*, and
262 *chr1* in Figure 4E. However, the relative eyespot positions within the cell differed. In the majority
263 of CC-3403 cells (~60%), the eyespot localized to an equatorial position. Approximately 35%
264 localized more anteriorly towards the flagella-bearing pole, while only ~5% localized towards the
265 posterior end. Both analyzed *chr2* strains had an identical distribution. In the *chr1* strains,
266 however, a clear tendency towards a predominantly anterior position was evident (~60%), and an
267 equatorial position was seen in only ~30% of the cells. Deletion of the last c-terminal 78 amino
268 acids (Figure 3B; ChR1:FLAG (Δ CT)) of ChR1 (Figure 4E; *chr1* Δ CT) had an identical effect. In
269 contrast, the *chr1 chr2* population exhibited an almost equal distribution of the eyespots between
270 these two positions and a slight increase in the posterior localization. Occasionally, two eyespots
271 were visible in *chr1 chr2* cells. Furthermore, malformed eyespots missing the typical roundish-
272 ellipsoid form were sometimes evident in *chr1* and *chr1 chr2* cells (Figure 4E). In addition, the
273 eyespot area was significantly smaller in the analyzed *chr1* and *chr1 chr2* strains compared to
274 CC-3403 (Figure 4F). In the other strains, no significant difference from the wild-type was

275 evident. These data indicate that ChR1 has a larger impact on eyespot plate positioning and
276 size/stability compared to ChR2. Furthermore, the observation that *chr1 chr2* forms visible, albeit
277 smaller eyespots supports the idea that additional eyespot proteins (EYE2 and others) are required
278 for the initial organization of the eyespot globule plate and that this process is ChR-independent
279 (Roberts et al. 2001; Boyd et al. 2011b; Mittelmeier et al. 2013).

280

281 Gene disruption using plasmid-encoded Cas9

282 Although our ZFN experiments enabled us to specifically modify target genes and respective
283 proteins at acceptable frequencies, it is difficult to design new ZFN pairs, and the number of
284 efficient target sites within a gene is limited. To develop a faster and more flexible gene-editing
285 approach, we endeavored to utilize the CRISPR/Cas9 system for targeting non-selectable genes in
286 *Chlamydomonas*. With functional Cas9 protein expression, only the guide RNA needs to be
287 adapted for any new GOI. Low target site restrictions (PAM) and easy guide RNA design
288 facilitate positional modifications.

289 A first prerequisite for CRISPR/Cas9 experiments is single guide RNA (sgRNA)
290 transcription under the control of an RNA polymerase III promoter (RNAPIII). In general,
291 RNAPIII transcription factor binding sites are inherent to the transcribed sequences, making them
292 unsuitable for sgRNA transcription. One of the few examples of sgRNAs with proximal RNAPIII
293 promoter elements is U6snRNA. Therefore, we employed a previously characterized U6snRNA
294 sequence from chromosome 8 (Jakab et al. 1997) and three other homologous CrU6snRNA
295 sequences of *C. reinhardtii*. The respective amplified promoter regions (500 bp) were used to
296 drive single-guide RNA transcription using the appropriate SaCas9 or SpCas9 scaffold sequences
297 (pCrU6#1-4//PmR; Fig 5A and Supplemental Table 2).

298 Disruption of the phytoene synthase-1 gene (*PSY1*) produces white colonies that are easy
299 to detect and count (Inwood et al. 2008; McCarthy et al. 2004). Therefore, we targeted the two
300 Cas9 variants to *PSY1* (*PSY1*-sg) to test promoter functionality. We chose a *PSY1* target site for
301 SaCas9 with a corresponding PAM (5`CGGAGT) that was also suitable for SpCas9 (5`CGG)
302 recognition. The transcription of *PSY1*-sg from each of the four different CrU6 sgRNA promoters
303 was tested in combination with either SaCas9 or SpCas9 expression (Fig 5A). CC-3403 cells were
304 electroporated with two separate circular plasmids, one containing a codon-optimized *Cas9* gene

305 and a second plasmid containing a U6-driven sgRNA gene and a PmR gene to allow for selection
306 of transformed cells. Cells were allowed to recover for 24 h at 22°C and selected on PmR. With
307 transformation conditions optimized for ZFNs, no white colonies were observed. However, we
308 detected a reasonable number of pale green colonies that were potentially derived from colonies
309 mixed with wild-type and *psy1* cells; such colonies were absent in the controls (Figure 5B).
310 Furthermore, extending the recovery time after electroporation from 24 to 48 h allowed us to
311 select white colonies. Among the CrU6 promoters examined, most white *psy1* colonies were
312 derived from the SaCas9/CrU6#4 electroporation (5 out of 56 PmR colonies; 9%). Increasing the
313 recovery temperature from 22°C to 33°C for 24 h, followed by 24 h at 22°C, further improved the
314 targeting efficiency (n=3; 16 ± 4%; Figure 5B). Exchanging the heat-shock inducible HSP70A
315 promoter with the constitutively active HSP70A/RBCS2 promoter (HR) led to the production of
316 fewer *psy1* clones (Figure 5B). SpCas9 created white colonies with reduced targeting frequencies
317 (2 out of 61 PmR colonies; 3.3%) compared with SaCas9. To characterize the modifications, the
318 *PSY1*-sg target site was PCR amplified and the product sequences were compared to wild-type
319 *PSY1*. In contrast to ZFN-modifications, most Cas9-modified *psy1* target loci were impossible to
320 amplify, possibly due to the large insertion size of plasmid DNA, as found by (Shin et al. 2016).
321 Of the white clones for which we obtained PCR products (7/96), three had 5–7 bp deletions
322 within the cleavage site, two potential siblings contained identical 25 bp deletions of *PSY1*
323 resulting from micro-homology-mediated end joining, and two contained inserted short fragments
324 of pHS_SaCas9 (Figure 5C). Based on these results, we determined that translated Cas9 was
325 active and that sufficient sgRNA was transcribed in CC-3403 cells to obtain clones with GOI
326 inactivation. The final transformation protocol for gene targeting using genetically encoded *Cas9*
327 and optimized conditions is illustrated in Fig 5D.

328 Using the optimized transformation conditions, we next disrupted photoreceptor genes that
329 were not expected to produce an immediate phenotype. For the four targeted photoreceptor genes
330 tested, *ChR2* (*ChR2*-sg), chlamyopsin-1/2 (*COP1/2*-sg), chlamyopsin-5 (*COP5*-sg), and
331 phototropin (*PHOT*-sg), we found target site insertions in the range of 2–10 kb (Figure 5E). The
332 insertion for the only phototropin disruption clone could not be amplified, but protein
333 immunoblotting confirmed the absence of PHOT protein in this mutant (Figure 5E). The two *cop5*
334 mutants (*cop5-1* and *cop5-2*) contained large but amplifiable fragments of *pCOP5*-sg (Figure 5F).
335 For SpCas9, the prolonged expression of the genome-integrated *Cas9* coding sequence was

336 hypothesized to cause cytotoxic effects (Jiang et al. (2014). We successfully amplified full-length
337 *SaCas9* DNA in 5 out of the 11 *SaCas9* modified strains tested (Figure 5G). For two of the
338 *SaCas9* amplicons from *cop5* clones, correct integration of the full-length *SaCas9* was confirmed
339 by sequencing. sgRNA sequences, including the CrU6#4 promoter, were supplied on the same
340 plasmid as the *aphVIII* selection marker and had integrated in all clones tested.

341 In summary, we disrupted four different photoreceptor genes in strain CC-3403 cells using
342 plasmid-based, genetically encoded *SaCas9*, and disruption efficiencies reached levels up to 9%
343 in preselected colonies.

344

345 **Gene disruption using preassembled Cas9/gRNA RNP complexes**

346 An alternative way to ensure the presence of functional CRISPR/Cas9 in cells is through direct
347 delivery of a ribonucleoprotein (RNP) complex with the Cas9 protein and synthetic CRISPR
348 RNA ((Kim et al. 2014). In *Chlamydomonas*, this delivery method has previously been used to
349 obtain mutants for phenotype screening (Baek et al. 2016; Shin et al. 2016). To enable easier
350 disruption of *Chlamydomonas* genes whose knockout would not create selectable or easily
351 scorable phenotypes, we modified the Cas9gRNA RNP technology to allow use of our mut-
352 *aphVIII* gene repair assay. CC-3403-GTS3 (Figure 2B) contains target sites for the well-
353 characterized human *EMX1* homeobox protein gene (Ran et al. 2015) and for ChR1-ZFNs. We
354 transformed the mut-*aphVIII* strain with *EMX1* SpCas/gRNA RNPs and HDR-repair donor
355 (pHDR-*APHVIII*^{A120}) (Figure 6A-B). On average, we obtained approximately 300 PmR colonies
356 with *EMX1* SpCas9/gRNA RNPs per 4 x 10⁶ electroporated cells compared with ~500 PmR
357 colonies from the ChR1-ZFN controls (Figure 6C). Omitting the pre-transformation heat shock
358 step reduced the number of PmR colonies 15-fold (21 PmR colonies). Increasing the temperature
359 from 22°C to 33°C for recovery after transformation did not alter the efficiency, unlike in the
360 plasmid-based system (Figure 6C).

361 Next, we targeted photoreceptor genes for which disruption strains were not yet available.
362 Based on our ZFN experiments, we created HDR donors with 30 bp unique sequence information
363 (FLAG) flanked by arms with homology to the target sequence, either as double-stranded
364 fragments (500-750 bp) cloned into plasmids or as ssODNs of 90 nt total length. The use of short
365 donors simplifies target site analysis because they allow for the detection of FLAG-PCR-based

366 integration or changes in target locus size by Locus PCR (Figure 6D). For our first candidate
367 gene, *aCRY*, we used a single donor spanning two adjacent target sites (Figure 6E). The *aCRY*-a
368 target site is located 24 bp upstream of the Flag integration site and is not destroyed by correct
369 FLAG integration, whereas *aCRY*-b is disrupted by the FLAG insertion. After transformation of
370 CC-3403 cells (which contain the *arg7* gene mutation) with Cas9/gRNA RNPs, plasmid donors,
371 and a WT *ARG7* marker gene, we analyzed 96 prototrophic clones for *aCRY*-a and *aCRY*-b target
372 site modifications. The *aCRY*-b gRNA apparently had little or no activity, because no arginine
373 prototrophic colonies containing *aCRY* gene modifications were obtained. However, we
374 successfully derived five mutants using a *aCRY*-a gRNA (Figure 6E). All five clones contained a
375 FLAG sequence integrated into the genome, but only one correct HDR mutant was found. The
376 four other clones had additional deletions within the remaining *aCRY*-a target site, possibly due to
377 multiple nuclease digestions (Figure 6E).

378 Next, we compared different donor species for the same target site within the *COP1/2*
379 gene, including plasmids, 90 nt ssODNs in PAM (NGG) or non-PAM (NCC) orientation, and 90
380 bp linear double-stranded templates (dsODNs) of complementary PAM and non-PAM ssODNs.
381 After transformation, 96 clones for each co-supplied HDR donor species were first screened by
382 FLAG-PCR. We found 6 HDR/NHEJ hybrid mutations with incorrect donor integration from
383 plasmid transformations (Figure 6E, i) and 10 hybrid mutations for 90 bp dsODNs (Figure 6E, iv)
384 with FLAG-inserts plus other mutations or insertions (e.g. duplications of the homology arms or
385 marker plasmid DNA fragments). Using Locus PCR, which is especially suited for detecting
386 insertions or deletions by NHEJ, we re-analyzed the same 96 clones and identified seven mutant
387 clones. Three of the HDR/NHEJ hybrids were also found by FLAG-PCR, but Locus PCR
388 identified four additional NHEJ mutants created by insertions of donor DNA or selection marker
389 plasmid fragments (Figure 6E, iv) (pHR11-Arg7). For PAM and non-PAM ssODN donors, we
390 found only a single mutant in each case, and only one of them contained a flawless FLAG
391 integration (Figure 6E *COP1/2* ii and iii).

392 Our data demonstrate that plasmids and ssODN HDR substrates create low amounts of
393 errorless knock-in mutants in conjunction with Cas9/gRNA RNPs, whereas short double-stranded
394 donors create higher numbers of unpredictable but valuable gene disruptions/modifications. Since
395 HDR integration of dsODNs could depend on the sequence context, we designed two gRNAs
396 each for *UVR8*, *COP5* (Histidine-kinase rhodopsin-1), and *VGCC* (voltage-gated calcium

397 channel) and used 90 bp dsODN templates. We analyzed 566 arginine prototroph colonies and
398 identified between 3 and 12 disruptions per target and 67 mutants in total (Figure 6F). However,
399 high gene disruption rates for dsODNs were only produced with HDR/NHEJ hybrids or NHEJ-
400 mutations, disqualifying dsODNs for use in HDR in *Chlamydomonas*.

401 For further in-depth characterization of the disruption mutants, we intend to perform
402 physiological assays and several imaging techniques, including super resolution microscopy and
403 cryo-electron tomography (Engel et al. 2015), all techniques for which cell wall-containing strains
404 are preferable. We repeated targeting of *COP5* and *VGCC* using the WT strain 137c (CC-125)
405 and *aCRY* using the WT strain SAG73.72. Additionally, we targeted *PHOT* and three non-
406 photoreceptor genes (*MAT3*, *KU80*, and *POLQ*) involved in cell cycle regulation and DNA repair
407 (Figure 6G). DSBs can be repaired by HR, by error-prone canonical NHEJ (supported by *KU80*),
408 or by alternative end joining mediated by the polymerase Theta *POLQ* (altEJ). Our data
409 demonstrated that the precise repair of Cas9-induced DSBs is a rare event and that mutated clones
410 that had undergone HR on one side of the break carried NHEJ/AltEJ-induced inserts of donor
411 DNA or random fragments of *Chlamydomonas* chromosome at the other side of the break. To
412 better understand the contribution of the NHEJ/AltEJ routes, especially for Cas9-induced gene
413 targeting, suppression of random insertions, and stimulation of HR, we generated *KU80* and
414 *POLQ*-deficient mutants for future analysis.

415 For an HDR template, we mixed two complementary PAM and non-PAM ssODNs
416 without annealing. We transformed CC-125 and SAG73.72 cells using adjusted electroporation
417 conditions and used the *aphVII* marker to preselect transformed cells for hygromycin resistance
418 (*HygR*). Locus- and/or FLAG-PCR revealed disruptions in all seven genes with frequencies
419 ranging from 1 (for *KU80-a*) to 14 (*PHOT-a*) out of 96 analyzed *HygR* colonies (Figure 6G).
420 Notably, for three target sites (*COP5-b*, *MAT3-a*, *PHOT-a*), we found 1-2 “clean” FLAG
421 insertions (Figure 6G, dark blue bars). Finally, we created a double knockout by transforming an
422 *uvr8* disruption strain with a Cas9/gRNA RNP and a plasmid bearing the *PHOT* template
423 sequence using *aphVIII* as a co-selection marker (Figure 6G). We confirmed the absence of
424 UVR8, COP1/2, and PHOT proteins from the respective deletion strains via protein
425 immunoblotting using available antibodies for these proteins (Figure 6H). Strain *phot-1* was
426 motile and tested for mating competence. *phot-1* cells mated reliably with CC-124 (137c(-)) cells
427 (Jun Minagawa, personal communication), challenging the previously drawn conclusion that

428 PHOT is needed for gamete formation (Huang and Beck 2003). The *mat3* mutant is defective in a
429 gene with strong homology to an animal retinoblastoma cancer gene involved in cell cycle
430 control. Our mutant showed the same small-size phenotype as related mutants originally created
431 by Gillham and colleagues via insertional mutagenesis (Gillham et al. 1987; Umen and
432 Goodenough 2001) (Figure 6I).

433 In conclusion, we optimized a method for direct transformation of preassembled
434 Cas9/gRNA RNP complexes into *Chlamydomonas* and disrupted eight different genes (*COP1/2*,
435 *COP5*, *aCRY*, *PHOT*, *UVR8*, *VGCC*, *MAT3*, *KU80*, *POLQ*) using four different strains (CC-3403,
436 CC-125, SAG73.72, 3403-*uvr8-2*) with various HDR donors (plasmids, ss- and dsODNs) and
437 three marker genes (*ARG7*, *aphVII*, and *aphVIII*). Figure 7 summarizes the workflows for all three
438 described nuclease systems with references to detailed descriptions in the Methods section.

439

440 DISCUSSION

441 In this study, we optimized several experimental parameters for more efficient application of ZFN
442 and Cas9-based gene-editing technology in motile *C. reinhardtii* cells, including the wild-type
443 strain CC-125 (Figure 7). The GTS system that we used for optimization has advantages over
444 most other monitoring assays, such as targeting selectable genes or phenotypic markers, because
445 it creates antibiotic-resistant clones after *aphVIII* repair by HDR. This allowed us to test and
446 quantify the activity of new nucleases and to compare different HDR donor designs and
447 transformation conditions.

448

449 Essentials for ZFN- and Cas9 mediated gene targeting

450 One of the most effective improvements to the ZFN approach is the change from glass-bead
451 transformation to electroporation. Although the overall DNA concentration for each plasmid used
452 in transformation remained constant (~30 ng/μl cell suspension), electroporation generated
453 approximately 50-fold more PmR colonies in the GTS system. Considering that 25-times fewer
454 cells (4x10⁶ cells) were employed for electroporation compared with glass beads (1x10⁸ cells), the
455 overall efficiency with respect to cell number increased by 1250-fold, with a value of up to 1

456 colony per 4000 transformed cells, which is a factor of ~100-fold above the previously reported
457 efficiency (Jiang and Weeks 2017).

458 In both plasmid-encoded nuclease systems (ZFNs and Cas9), increasing the recovery
459 temperature to 33°C was beneficial for targeting events, but it did not affect the efficiency of
460 recombinant Cas9/gRNA RNP s. We used the HSP70A promoter, which was previously
461 characterized using a limited heat-shock period of 30 min at 40°C, yielding high levels of protein
462 expression after 60 min (Schroda et al. 2000). Our studies demonstrated that increasing the
463 recovery temperature to 33°C for 24 h post-transformation allowed for continued transcription
464 from this promoter and was a good compromise between high protein expression and survival
465 rate. Most critically, we expect that the 30 minute heat-shock treatment applied pre-
466 transformation is one (if not the only) essential parameter for the superior efficiency compared to
467 previous reports (Shin et al. 2016; Jiang and Weeks 2017). Heat shock treatment prior to
468 transformation induces unknown physiological changes that are favorable to Cas9/gRNA activity
469 and/or to processes involved in DNA repair (Figure 6C), DNA integration and/or homologous
470 recombination that merit future investigation.

471

472 **Activity of genetically encoded Cas9**

473 We demonstrated that Cas9 can be expressed in *C. reinhardtii* in sufficient amounts to generate
474 mutants with or without integration of the *Cas9* coding DNA into the genome (Figure 5G). There
475 are two main factors that may have prevented earlier establishment of this plasmid-based
476 CRISPR-Cas9 system. First, the use of standard transformation conditions, including a recovery
477 time of 24 h at 22°C before plating, results in the production of mixed non-homogenous colonies
478 due to delayed Cas9 expression (Kouranova et al. 2016), as we demonstrated in the *PSYI*
479 disruption experiments. Second, *C. reinhardtii* exhibits atypical gene modification preferences.
480 Although small insertions/deletions are pre-dominant in other systems (Zheng et al. 2016; Zhu et
481 al. 2017), most *Chlamydomonas* mutants have acquired large insertions that are difficult to
482 analyze and might have remained undetected or disregarded during analysis (Shin et al. 2016).
483 Additional experiments are needed to determine if any HDR donors (e.g. PTO-protected HDR
484 substrates) can remain un-degraded long enough for Cas9 translation to peak and further increase
485 the number of mutants obtained. Irrespective of the gene-editing method utilized, the adaptation

486 of this technology to *Chlamydomonas* can serve as a basis for improving other Cas9 applications,
487 such as gene activation/repression (Kao and Ng 2017).

488

489 **ZFN and Cas9 favor different repair mechanisms**

490 HDR is approximately ten-times less likely after DNA cleavage with Cas9 compared to ZFN.
491 Moreover, the ratio of HDR to NHEJ/alternative end joining (altEJ; (Ceccaldi et al. 2016) differed
492 significantly, even though ZFNs and recombinant Cas9 created nearly equal numbers of PmR
493 colonies. ZFNs created DSBs that were repaired via HDR in most isolated clones with all donor
494 types we tested. In contrast, in the Cas9 experiments, we found that short double-stranded HDR-
495 donors tended to create multiple insertions. This observation is in accordance with the creation of
496 blunt cuts, a longer dwell time on DNA, and a delayed release of one DNA strand after cleavage
497 by Cas9 (Sternberg et al. 2014). These differences might prevent perfect integration of symmetric
498 HDR donors and promote non-homologous integration of double-stranded templates.
499 Nevertheless, HDR via Cas9 is possible in *C. reinhardtii*. Suppression of NHEJ was achieved
500 using single-stranded DNA templates, but in this case, the number of clones with HDR-based
501 GOI modification was again small. Alternatively, the disruption of *KU70/KU80* or *POLQ* or the
502 inhibition of Ligase IV by SCR7 could be used to suppress NHEJ/altEJ of double-stranded donors
503 (Chu et al. 2015). The *ku80* and *polq* strains are currently available for such experiments (Figure
504 6G).

505 In future experiments in *C. reinhardtii* and related green algae, our results suggest that
506 Cas9 DNA or protein should be used in combination with small PTO-protected double-stranded
507 HDR donors for rapid, efficient gene disruption. However, for clean and predictable gene
508 modification, ZFNs may be preferable for use in combination with larger plasmid donors (≥ 750
509 bp).

510

511 **Advantage of direct gene modification in *C. reinhardtii***

512 For the generation of gene modifications, direct gene targeting is an efficient alternative to
513 screening of insertion libraries, a current widely used technology in cases where deletion mutants
514 are required or requested (Galvan et al. 2007; Li et al. 2016) (Cheng et al. 2017). Insertion

515 mutagenesis has the advantage that thousands of mutants are generated simultaneously. However,
516 marker DNA is inserted randomly and most frequently into introns; genes are not necessarily
517 inactivated, and insertions within the GOI are still laborious to detect in most cases. By contrast,
518 gene deletion using Cas9 is fast, occurs specifically at the site of interest, and is cost effective. A
519 handful of mutants can be retrieved from a single 96 well plate, which supports the interpretation
520 of subsequent physiological experiments. This indicates that mutants can be produced on demand,
521 preventing the need for expensive library maintenance. The technology can be scaled up or
522 multiplexed, as shown for mammalian cell lines, where >18,000 genes were inactivated in parallel
523 using >64,000 gRNAs in a single experiment (Shalem et al. 2014). Finally, direct gene targeting
524 by ZFN or Cas9 separates the selection marker from the targeting site, enabling outcrossing of the
525 marker and sequential inactivation of many genes applicable to any strain of choice.

526

527 **Channelrhodopsin physiology**

528 By disrupting *ChR1* and *ChR2* in CC-3403, we demonstrated that precise modification of non-
529 selectable genes in wild-type-like, motile *C. reinhardtii* cells is possible. We performed careful
530 physiological characterization of single and double knockout lines of *ChR1* and *ChR2* and
531 confirmed that ChR1 and ChR2 are the sole photoreceptors for phototaxis in *C. reinhardtii*, as
532 previously determined using antisense experiments (Sineshchekov et al. 2002; Berthold et al.
533 2008). The availability of clean disruption mutants allowed us to quantify the relative contribution
534 of ChR1 and ChR2, which is approximately 100:1 in CC-3404 gametes. The mislocalization of
535 ChR1 after tagging with mCherry (Figure 4D) suggests that an undisturbed C-terminus is
536 necessary for its targeting and/or transport to the eyespot along the four-membered microtubule
537 rootlet (D4) (Mittelmaier et al. 2011; Awasthi et al. 2016). Using the *ChR1* and *ChR2* mutants, we
538 determined that the ChR patch and eyespot globule layers can assemble independently. In
539 addition, assembly of a functional eyespot is dependent on the chloroplast envelope protein
540 EYE2, which nucleates the formation of the carotenoid-rich eyespot globule layers (Boyd et al.
541 2011b; Boyd et al. 2011a; Mittelmeier et al. 2013). Our data demonstrate that the EYE2 patch and
542 visible eyespots form independently of the ChRs. However, the reduction in eyespot size and the
543 observed malformed eyespots in *chr1* and *chr1 chr2*, but not in *chr2* or *chr1Δct*, suggest that
544 ChR1 may stabilize the eyespot globule plate. Furthermore, low levels of ChRs or ChR1 without

545 a full C-terminus were not sufficient for the retention of a normal dominating equatorial eyespot
546 position, supporting the hypothesis of Mittelmeier et al. (2013) that eyespots will be more anterior
547 in the absence of ChRs compared to wild-type cells. The ChR mutants generated here lay the
548 foundation for further characterization of phototaxis and behavioral physiology. Moreover, our
549 optimized methods can be used to generate additional ChR mutants with altered absorption,
550 kinetics, ion selectivity, and adaptation to variable light conditions (Schneider et al. 2015). These
551 ChR mutants will be of great value to the *Chlamydomonas* field for understanding ChR transport,
552 as well as eyespot assembly, positioning, and size/stability control.

553

554 METHODS

555 Sections 1–5 below are arranged in accordance with the workflow scheme in Figure 7. Methods
556 used for preliminary experiments of specific analytic studies not necessarily recommended for
557 users are described at the end of this section.

558 1. Strain and culture conditions

559 Motile *Chlamydomonas reinhardtii* strains CC-3403 (RU-387 *nit1 arg7 cw15 mt-*), CC-503
560 (*cw92 mt+*), CC-125 (137c *nit1 nit2 agg1+ mt+*) were obtained from the Chlamydomonas
561 Resource Center (<http://www.chlamycollection.org>) and SAG73.72 (*mt+*) was obtained from
562 Maria Mittag (Friedrich Schiller University Jena). Cells were grown in standard Tris-acetate-
563 phosphate (TAP) medium (Gorman and Levine 1965), optionally supplemented with 100 µg/ml
564 L-arginine (TAP-Arg) under continuous cool fluorescent white light of 40–60 µE m⁻² s⁻¹ at 110
565 rpm at 22°C or alternatively for synchronized cultures in cycles of 14 h at 25°C under light and 10
566 h at 18°C in darkness.

567

568 2. DNA preparation and Cas9 protein purification

569 Circular plasmid DNA used for *Chlamydomonas* transformation was isolated from XL-1 blue
570 *Escherichia coli* cells and column purified according to the manufacturer's instruction (Machery-
571 Nagel NucleoSpin Plasmid EasyPure).

572

573 *Streptococcus pyogenes* Cas9 protein was expressed and purified as described (Gagnon et al.
574 2014). Briefly, the Cas9 expression plasmid pET-28b-Cas9-His (Addgene plasmid # 47327) was

575 transformed into *E. coli* strain Rosetta2(DE3). The Cas9-expressing clone was grown in 500 ml
576 LB medium with 100 mg/ml ampicillin at 37°C for 2 h before induction with 1 mM IPTG.
577 Expression was carried out overnight at 25°C. *E. coli* cells were resuspended in lysis buffer (20
578 mM Tris [pH 8.0], 300 mM NaCl, 10 mM imidazole, DNaseI, 0.1 mM PMSF) and lysed using an
579 EmulsiFlex-B15 homogenizer (Avestin). The lysate was purified by immobilized affinity
580 chromatography (5 ml nickel column FF-Crude, Desalt 16-60 GE Healthcare). Protein
581 concentration was determined by A260/A280 absorption, diluted to 10 µM (~3.1 µg/µl) in 1x
582 Buffer O (BO5, Thermo Fisher Scientific Inc.), and filter sterilized, and aliquots were shock
583 frozen in liquid nitrogen and stored at -80°C.

584

585 **3. Transformation of *C. reinhardtii* cells**

586 **3.1. Cell growth, heat shock, and transformation**

587 Cells were grown under a synchronized light (14 h, 25°C) / dark (10 h, 18°C) cycle for at least 10
588 days and kept in exponential growth phase by diluting 1:50 every 3-4 days with fresh TAP(-Arg)
589 medium. However, strictly speaking, whether or not synchronization of the algal culture has an
590 effect on gene targeting efficiency has not been determined for the final recipe, and
591 transformation of non-synchronized cells might work equally well.

592 Cells at a density of $1\text{-}3 \times 10^6$ cells/ml were harvested by centrifugation at $2000 \times g$ for 10
593 min at room temperature (RT) and resuspended in TAP medium supplemented with 40 mM
594 sucrose (TAP-Suc) for ZFN and Cas9 plasmid-based experiments. For Cas9 protein experiments,
595 cells were resuspended in MAX Efficiency transformation medium (A24229, Thermo Fisher
596 Scientific Inc.) supplemented with 40 mM sucrose (ME-Suc) to a density of 1×10^8 cells/ml.
597 Prior to transformation, concentrated cells were heat shocked at 40°C for 30 min in a
598 thermomixer (Eppendorf) operated at 350 rpm. Procedures were timed in such a way that the cells
599 were actually electroporated with nucleases (see below) -2 h to +2 h after entering the dark phase.
600 Transformation was carried out by electroporation using a NEPA21 electroporator (Nepa Gene
601 Co., Ltd., Japan) according to the manufacturer's instructions and Yamano and colleagues
602 (Yamano et al. 2013). The impedance of a 40-µl cell suspension (4×10^6 cells) should be 400–550
603 ohms; if not, the volume was adjusted by withdrawing or adding 5 µl cell suspension. CC-3403
604 and CC-503 cells were electroporated using two 8-ms/200-V poring pulses at 50-ms intervals and
605 a decay rate of 40%, followed by five 50-ms/20-V polarity-exchanged transfer pulses at 50-ms

606 intervals and a decay rate of 40%. CC-125 and SAG73.72 cells were electroporated using one 8-
607 ms/300-V poring pulses at 50-ms intervals and a decay rate of 40%, followed by five 50-ms/20-V
608 polarity-exchanged transfer pulses at 50-ms intervals and a decay rate of 40%.

609

610 3.2. Nucleases

611 **Zinc-finger nucleases (ZFN; Figure 7A):** For targeting the channelrhodopsin-1 (*ChR1*) gene,
612 ZFNs were used as described previously (Sizova et al. 2013). To target *ChR2*, designed ChR2-a-
613 ZFNs were designed using the ZiFit database. Sigma-Aldrich (CompoZr) designed and
614 functionally evaluated the ChR2-b-ZFNs. An N-terminal Simian Virus 40 nuclear localization
615 signal (MAPKKKRKVGIHG) was added and the ZF-binding domains were fused to the *FokI*
616 nuclease domain. ZFN expression was controlled by the HSP70A promoter (Schroda et al. 2000)
617 and transcription termination regulated by the 3' region of *RBCS2*. Sequences were codon-
618 optimized for expression in *C. reinhardtii* and synthesized by Genescript. Plasmid maps are
619 provided in Supplemental Table 1. 1 µg of each ZFN plasmid (left and right, pZFN-L and pZFN-
620 R), 0.3 µg of marker plasmid pHRI1(*ARG7*) and 2 µg of pHDR donor plasmids (all circular)
621 were used per transformation.

622

623 **Plasmid-encoded Cas9 (Figure 7B):** *Staphylococcus aureus* Cas9 (SaCas9) and *Streptococcus*
624 *pyogenes* Cas9 (SpCas9) coding sequences were codon optimized to the average *C. reinhardtii*
625 codon bias and ordered from a commercial supplier (GenScript). Sequences 3' of the HSP70A or
626 HSP70A/RBCS2 promoter were cloned (Schroda et al. 2000). Fully annotated plasmid maps are
627 provided in Supplemental Table 2, including nuclear localization signals. *Chlamydomonas* U6
628 promoters for *in vivo* single guide RNA (sgRNA) transcription were identified by BLAST
629 searching the published U6 small nuclear RNA (snRNA) sequence (Jakab et al. 1997) against the
630 *C. reinhardtii* genome (Phytozome v11). Four promoters were chosen, and synthetic double-
631 stranded DNA fragments (Integrated DNA Technologies; gblocks) were ordered for the U6
632 promoter sequences, followed by two *Esp3I* restriction sites and the corresponding SaCas9 or
633 SpCas9 sgRNA scaffold. The *Esp3I* restriction sites were inversely positioned following the
634 protocol of Ran et al. (Ran et al. 2013) to create a specific 4-bp overhang after cleavage to allow
635 for insertion of the protospacer sequence as annealed oligos in a cut-ligation reaction (for details,
636 see Supplemental Table 3 and 4). The immediate 4-bp sequence upstream of the transcriptional

637 start site was changed to ACTT in all U6 constructs to simplify the cloning procedures. For the
638 electroporation transformation reactions, 2 µg of non-linearized Cas9 plasmid and 1 µg of sgRNA
639 coding plasmid were used. For experiments involving the use of a donor DNA, 1 µg of plasmid
640 was added. All plasmids and corresponding maps used for the Cas9 experiments are provided in
641 Supplemental Table 2.

642

643 **Recombinant Cas9 ribonucleoprotein (RNP; Figure 7C):** Recombinant *Streptococcus*
644 *pyogenes* Cas9 protein was complexed with guide RNA (gRNA), forming a ribonucleoprotein
645 (RNP). gRNAs were ordered as two RNAs, the scaffold RNA (tracrRNA) with constant
646 sequence, and the target sequence (crRNA), which differed for each target site, according to the
647 guidelines of a commercial supplier (Alt-R CRISPR-Cas9 system, Integrated DNA
648 Technologies). All RNAs and target (protospacer) sequences are shown in Supplemental Table 5.
649 Equimolar amounts of tracrRNA and crRNA (Figure 6A) were annealed in DUPLEX buffer (100
650 mM potassium acetate, 30 mM HEPES, pH 7.5; Integrated DNA Technologies) to a final
651 concentration of 10 µM by heating to 95°C for 2 min, followed by cooling at a rate of 0.1°C/min.
652 Purified 10 µM Cas9 protein was mixed with equimolar amounts of annealed gRNA in 1× Buffer
653 O (BO5, Thermo Fisher Scientific Inc.) to a final concentration of 3 µM each and incubated for
654 15 min at 37°C. Assembled Cas9/gRNA RNP were kept on ice until the next experiment or
655 stored at 4°C for up to one week. Cells were mixed with 2–5 µl of 3 µM Cas9 RNP, 10-20 pmol
656 of ss- or ds-HDR ODNs or 2 µg of pHDR donor plasmid, and 0.3 µg selection marker plasmid
657 pHR11(ARG7), pAphVII or pAphVIII. The resistance of transformation mixtures in
658 electroporation cuvettes was carefully monitored and maintained at 0.3–0.7 kOhm by adding or
659 withdrawing 5 µl to the cell-RNP-DNA mixture.

660

661 **3.3. Homology-directed repair (HDR) donors**

662 Three classes of HDR donors were used: linear single-stranded oligonucleotides, linear double-
663 stranded DNA, and plasmids. These classes all had the integration of a 28-32 bp FLAG insert
664 interspersing the cutting site in common. This “FLAG” sequence contains an in-frame stop codon
665 and alters the reading frame. The “FLAG” sequences used in the study are listed in Supplemental
666 Table 6. Oligonucleotides: single-stranded (ss) 90-bp oligos were ordered with 2–3
667 phosphorothioate (PTO) bonds at the 3' and/or 5' end bases. In the case of short double-stranded

668 (ds) HDR donors, 100 μ l 20 μ M equimolar sense and antisense oligonucleotide were annealed in
669 1 \times duplex buffer (100 mM potassium acetate, 30 mM HEPES, pH 7.5; Integrated DNA
670 Technologies, Coralville) by incubating at 95°C for 2 min, followed by cooling at a rate of
671 0.1°C/min. A total of 10 pmol of ss or annealed ds oligos were used per transformation. PCR
672 products (Figure 2D): Donor sequences of 500 bp were amplified with 5'PTO-protected
673 oligonucleotides. A total of 500–1000 ng of purified PCR product was used per transformation.
674 Plasmids: Donor sequences of 500–3000 bp with a FLAG insert were ordered as gBlocks or
675 generated via overlapping PCR and cloned blunt-ended into pBluescript KS(–) vectors. A total of
676 1–2 μ g circular donor plasmid was used per transformation. All donor sequences are listed in
677 Supplemental Table 7 and 8.

678

679 **3.4. Selection markers**

680 The Streptomyces aminoglycoside-5'-phosphotransferase *aphVIII* selection marker (Sizova et
681 al. 2001) was used in all experiments involving plasmid-encoded Cas9 and in double knockout
682 experiments. The marker was either cloned into the sgRNA plasmid or co-transformed as a
683 separate plasmid along with other plasmids. pHRI1(*ARG7*), a gift kindly provided by Hussam
684 Hassan Nour-Eldin (Chlamydomonas Resource Center #pHR11), was used to reconstitute
685 arginine auxotrophy in ZFN and Cas9 RNP experiments with strain CC-3403. pAphVII (Berthold
686 et al. 2002) gives resistance to Hygromycin B and was used to transform CC-125 cells. If GTS
687 strains were complemented with donor DNA, no additional marker was used. Plasmids and
688 corresponding maps are listed in Supplemental Table 1.

689

690 **4. Recovery, plating, and picking**

691 After electroporation, the cells were diluted in 500 μ l of TAP(-Arg) and incubated at 22°C or
692 33°C for 24 h for ZFNs, 33°C for 24 h plus 22°C for another 24 h for plasmid *Cas9*, or 22°C for
693 24 h prior to plating for Cas9/gRNA RNP. After incubation, the cell suspensions were transferred
694 to agar plates. In the case of paramomycine selection via *aphVIII*, plates contained 10 μ g/ml of
695 paromomycin; for Hygromycin selection via *aphVII*, plates contained 10 μ g/ml of Hygromycin B,
696 and for *ARG7* selection, arginine-free agar plates were used. Colonies appeared after 7–10 days
697 and were picked with sterile toothpicks and transferred to 96-well plates containing 180 μ l of
698 TAP-Arg.

699

700 **5. Screening procedures**

701 **5.1. Crude cell extracts**

702 PCR amplification of genomic *Chlamydomonas* DNA was performed in a 96-well format using
703 Phire Plant Direct PCR Master Mix (Thermo Fisher Scientific Inc., dilution buffer protocol).
704 Cells were grown in 180 µl of TAP-Arg medium in 96-well plates until all wells turned uniformly
705 green. A 40-µl aliquot of each cell culture was then transferred to a 96 well V-bottom culture
706 plate and centrifuged at 2000 × g for 10 min at RT (22°C). The supernatant was removed and the
707 pellet thoroughly resuspended in 20 µl of dilution buffer, incubated for 5 min at RT (22°C), and
708 centrifuged again at 4000 × g for 10 min at RT; 80 µl of ddH₂O was added carefully to the
709 supernatant, avoiding cell pellet resuspension. This step is optional but we found higher dilution
710 of genomic DNA from dilution buffer extractions work more reliably possibly due to lower
711 amounts of inhibitory compounds from plant material. PCR was carried out according to the
712 manufacturer's instructions. A total of 0.5–2 µl of DNA extract solution was used for a 10-µl
713 PCR reaction, containing 10 pmol oligonucleotides, 1 M betaine, and 1× Phire Plant Master Mix.
714 Typically, an initial denaturation (5 min, 98°C) was followed by 30-35 cycles of denaturation (10
715 sec, 98°C), annealing (10 sec, 60-72°C) and elongation (20-200 s, 72°C) with a final elongation
716 (2 min, 72°C). Oligonucleotides with 25-30 bp were designed with a melting temperature of 60-
717 65°C and tested before screenings. A PerfectBlue Maxi ExW electrophoresis system (Peqlab,
718 VWR) was used to analyze the amplicons from the 96-well PCR plates with 1–3% Tris-borate-
719 EDTA agarose gels. For PCR products of 300 - 2000 bp, crude cell extracts were used instead of
720 whole cells. All oligonucleotide sequences used for screening are listed in Supplemental Table 6.

721

722 **5.2. Whole-cell qPCR**

723 Due to the high failure rate in *psy1* locus amplification, we reasoned that most Cas9 target sites
724 contain large insertions from electroporated plasmid DNA. Therefore, our screening strategy was
725 changed from a single-stage conventional PCR to a double-stage qPCR/long range PCR protocol.
726 First, qPCR was applied to genomic DNA from selected clones using short elongation times of 20
727 s. All corresponding clones that failed in qPCR target locus amplification were subjected to a
728 conventional long-range PCR elongation time of 300 s. Isolated colonies (1–2 mm diameter) were
729 picked and transferred into 180 µl of TAP medium in a 96-well plate. The plates were

730 immediately processed for qPCR, or the cells were allowed to grow overnight. However, further
731 growth should be avoided, as most qPCR mixes are sensitive to inhibitors from plant materials. In
732 preliminary tests, we found SsoAdvanced Universal SYBR Green Supermix (Bio-Rad) or SsoFast
733 Evagreen Supermixes (Bio-Rad) were most reliable for amplification of genomic *C. reinhardtii*
734 template DNA. 1.5 µl of the 180 µl cell suspension was used for a 10-µl qPCR reaction mixture
735 including 10 pmol of each oligonucleotide, 1 M betaine (final concentration), 1× Mastermix.
736 Cycling protocol: initial denaturing step of 5 min at 98°C; 40 amplification cycles: 98°C for 10 s,
737 60–65°C for 20 s. Oligonucleotides for locus PCR were chosen to create a product in the range of
738 150–300 bp. *COP1* forward and reverse oligonucleotides (COP1-F and COP1-R Supplemental
739 Table 4) were used as a control in different GOI targeting experiments because they facilitate
740 reliable amplification over the range of 60–72°C for annealing/elongation. PCR was carried out
741 using a CFX-Connect cycler (Bio-Rad). Melting curves were recorded using 0.2–0.5°C steps,
742 depending on the expected product size differences. For FLAG PCRs and LOCUS PCR, the
743 respective oligonucleotide pairs must be used, as explained in Figure 7.

744

745 **Creating GTS strains**

746 A 40-45-µl volume of concentrated cell culture (1×10^8 cell/ml; CC-3403) was mixed with 500 ng
747 of linearized pGTS plasmid DNA. After transformation, the cells were allowed to recover
748 overnight in 0.5 ml of TAP medium under continuous light at RT (GRO LUX WIDE, $280 \mu\text{E m}^{-2}$
749 s^{-1} , 22°C). The next day, cells were plated on TAP agar plates containing 10 µg/ml of Zeocin™
750 (Invitrogen). After 10–14 days, colonies were picked and analyzed under a microscope for signs
751 of motility. Complete integration of the GTS cassette was tested in motile cells with
752 oligonucleotide Ble-Starfw and 3'Psa-467rev. For further experiments, 2-8 potential GT strains
753 were tested using the *aphVIII* repair assay with *ChR1*-ZFNs, which are known to be functional.

754

755 **mut-*aphVIII* repair assay transformations**

756 1 µg of each ZFN plasmid (left and right) or 6 pmol *EMX1* Cas9/gRNA RNP and 2 µg of pHDR-
757 *APHVIII*^{Δ120} (all circular) were used per transformation. Unless specified differently, a heat shock
758 (40°C, 30 min) was applied before transformation and cells were recovered at RT (22° C) for 24
759 h. Cells were plated and selected on paromomycin (10 µg/ml). Colonies appeared after 8–10 days
760 and were counted from photographs of plates using OpenCFU software (Geissmann 2013).

761

762 ***PSY1*, *COP1*, *VGCC*, *COP5*, and *PHOT* deletion experiments**

763 The sequence of each gene was examined for suitable Cas9 target sites using Benchling software
764 (benchling.com), in which the *C. reinhardtii* genome is integrated to evaluate off-targeting. In the
765 case of SaCas9 experiments, the NNGRRT protospacer adjacent motif (PAM) was always
766 chosen, except for phototropin, which had an NNGRR PAM (Ran et al. 2015). All protospacers
767 had on-target scores of ≥60 (Doench et al. 2014). Detailed protospacer sequences, plasmid maps,
768 and gene IDs are provided in Supplemental Table 3. Because *PSY1* deletion mutants are light
769 sensitive, these cells were always kept in the dark. The pre-plating incubation temperature was
770 either 33 or 22°C for 24 h, followed by 24 h at 22°C. After incubation, the cells were plated on
771 TAP agar plates containing 10 µg/ml of paromomycin. In the case of *PSY1*, 0.3% (w/v) yeast
772 extract and 0.2% (w/v) tryptone was added to the agar plates to enhance growth in darkness.
773 Single colonies were obtained after approximately 2 weeks. *PHOT*-deletion mutants had to be
774 selected under dim light conditions of 20 µE m⁻² s⁻¹. After colony picking, the clones only grew
775 under a light/dark regime.

776

777 **Protein analysis**

778 Proteins were separated by sodium dodecyl sulfate–polyacrylamide gel electrophoresis using 4–
779 15% Mini PROTEAN TGX precast protein gels (Bio-Rad) and transferred onto low-fluorescence
780 polyvinylidene difluoride membranes using a Trans-Blot® Turbo transfer system (Bio-Rad). Blots
781 were incubated overnight with anti-LOV1 (1:2000), anti-VOP (1:2000) or anti-UVR8 (1:2000), or
782 affinity-purified anti-ChR1 (1:500) or anti-ChR2 (1:500) rabbit polyclonal antibodies. Secondary
783 antibodies were allowed to bind for 2 h (horseradish peroxidase-conjugated ECL anti-rabbit IgG
784 [donkey]; GE Healthcare, NA934V). Clarity ECL Western substrate-induced luminescence was
785 detected using the ChemieDoc MP system (Bio-Rad).

786

787 **Phototaxis Assay**

788 Phototactic orientation was measured in a custom-made light-scattering apparatus (Berthold et al.
789 2008; Uhl and Hegemann 1990). In brief, cells were transferred to NMM medium (80 μ M
790 MgSO₄, 100 μ M CaCl₂, 3.1 mM K₂HPO₄, and 3.4 mM KH₂PO₄, pH 6.8) two days before
791 experiments to induce gametogenesis. Infrared measuring light was scattered by a
792 *Chlamydomonas* suspension (1×10^6 /ml) onto infrared sensitive photodiodes. The current
793 produced by the IR diode is proportional to the intensity of the scattered light and gives a measure
794 of its orientation towards a perpendicular monochromatic light. For excitation, LEDs of 455 nm
795 (10 μ E m⁻²s⁻¹) and 530 nm (10 μ E m⁻² s⁻¹) were used and light intensities were adjusted using
796 neutral-density filters.

797

798 **Microscopy**

799 Color photographs of unfixed cells were taken with an Axioimager M2 (Zeiss, 63 x
800 PlanApoChromat 1.4–numerical aperture oil immersion objective; DIC) equipped with an
801 AxioCam ERc5S camera (Zeiss). Cells for eyespot area measurements, position, and cell length
802 determinations were analyzed as described in detail by Trippens et al. (2012) using an Eclipse 800
803 microscope (Nikon, Plan Apo 100 x, 1.4–numerical aperture oil immersion objective) and DIC
804 microscopy. NIS-Elements software (Nikon) was used for measurements, and statistical analyses
805 were done using GraphPad Prism 5 software. Parameters and results of ANOVA and multiple
806 comparison test are listed in Supplemental Table 9. Live cell imaging of mCherry-expressing
807 strains was carried out using an Olympus FV1000 confocal microscope equipped with an Uplapo
808 60 x W (NA: 1.20) objective and appropriate filter sets.

809

810 **Accession numbers**

811 The accession numbers for all *Chlamydomonas* genes are provided in Figure 1 and Supplemental
812 Table 3 and 5.

813

814 **Supplemental Data**

815 **Supplemental Table 1.** Plasmids used for zinc-finger nuclease experiments.

816 **Supplemental Table 2.** Plasmids used for the CRISPR-Cas9 experiments.

817 **Supplemental Table 3.** Protospacer sequences and target gene information.

818 **Supplemental Table 4.** Oligos used for protospacer insertion.

819 **Supplemental Table 5.** crRNAs used for recombinant Cas9 transformations.

820 **Supplemental Table 6.** Oligonucleotides used for cloning, screening, and HDR-donor

821 amplification.

822 **Supplemental Table 7.** Oligonucleotides used as HDR-Donors.

823 **Supplemental Table 8.** gBlocks ordered as HDR-templates.

824 **Supplemental Table 9:** Statistical analysis for Figure 4F.

825
826 All plasmids, primers, guide RNAs and HDR donors are listed in the Supplemental Tables with
827 hyperlinks to fully annotated plasmid maps.

828
829 **ACKNOWLEDGMENTS**
830 We thank Margret Michalsky, Thi Bich Thao Nguyen, Mirjam Langenegger, and Francisca
831 Boehning for excellent technical assistance; Wenshuang Li and Patrick Segelitz for isolating the
832 aCry disruption mutants; Suneel Kateriya and Lina Sciesielski for fruitful discussions; Roman
833 Ulm for supplying the UVR8 antibody; Richard Chappuis for immunoblot analysis of our *UVR8*
834 knockouts and Jun Minagawa for the *phot-1* mating assay. We also thank the Benchling team for
835 integrating the *Chlamydomonas* genome into the CRISPR/Cas9 guide RNA design tool upon
836 request.

837 This work was supported by the German Research Foundation, DFG (FOR1261 and Leibniz
838 grant) and by the Russian Foundation for Basic Research (grant 17-54-45088, to I.S.). P.H. is a
839 Hertie Senior Professor for Neuroscience supported by the Hertie Foundation.

840

841 **AUTHOR CONTRIBUTIONS**

842 P.H., I.S., and A.G. designed the experiments; I.S. and A.G. developed the GTS system; and I.S.
843 designed the ZFNs. S.K. established the ZFN protocols. A.G. established the plasmid-based Cas9
844 and screening protocols. S.K. established the recombinant Cas9 protocols. H.E. made the DNA
845 constructs and selected and characterized the clones. G.K. analyzed cell shape and eyespot
846 positioning by microscopy. A.G. and P.H. wrote the manuscript, with input from I.S., S.K., and
847 G.K.

848

849

850 **REFERENCES**

- 851
- 852 Baek K, Kim DH, Jeong J, Sim SJ, Melis A, Kim JS, Jin E, Bae S (2016) DNA-free two-gene
853 knockout in *Chlamydomonas reinhardtii* via CRISPR-Cas9 ribonucleoproteins. *Scientific*
854 *reports* 6:30620. doi:10.1038/srep30620
- 855 Beel B, Prager K, Spexard M, Sasso S, Weiss D, Muller N, Heinrichs M, Dewez D, Ikoma D,
856 Grossman AR, Kottke T, Mittag M (2012) A flavin binding cryptochrome photoreceptor
857 responds to both blue and red light in *Chlamydomonas reinhardtii*. *Plant Cell* 24 (7):2992-
858 3008. doi:10.1105/tpc.112.098947
- 859 Berthold P, Schmitt R, Mages W (2002) An engineered *Streptomyces hygroscopicus* aph 7" gene
860 mediates dominant resistance against hygromycin B in *Chlamydomonas reinhardtii*.
861 *Protist* 153 (4):401-412. doi:10.1078/14344610260450136
- 862 Berthold P, Tsunoda SP, Ernst OP, Mages W, Gradmann D, Hegemann P (2008)
863 Channelrhodopsin-1 initiates phototaxis and photophobic responses in *Chlamydomonas*
864 by immediate light-induced depolarization. *Plant Cell* 20 (6):1665-1677. doi:Doi
865 10.1105/Tpc.108.057919
- 866 Bibikova M, Beumer K, Trautman JK, Carroll D (2003) Enhancing gene targeting with designed
867 zinc finger nucleases. *Science* 300 (5620):764. doi:10.1126/science.1079512
- 868 Boyd JS, Mittelmeier TM, Dieckmann CL (2011a) New insights into eyespot placement and
869 assembly in *Chlamydomonas*. *BioArchitecture* 1:196-199. doi:10.4161/bioa.1.4.17697
- 870 Boyd JS, Mittelmeier TM, Lamb MR, Dieckmann CL (2011b) Thioredoxin-family protein EYE2
871 and Ser/Thr kinase EYE3 play interdependent roles in eyespot assembly. *Mol Biol Cell* 22
872 (9):1421-1429. doi:10.1091/mbc.E10-11-0918
- 873 Braun FJ, Hegemann P (1999) Two light-activated conductances in the eye of the green alga
874 *Volvox carteri*. *Biophys J* 76 (3):1668-1678
- 875 Ceccaldi R, Rondinelli B, D'Andrea AD (2016) Repair Pathway Choices and Consequences at the
876 Double-Strand Break. *Trends Cell Biol* 26 (1):52-64. doi:10.1016/j.tcb.2015.07.009
- 877 Cheng X, Liu G, Ke W, Zhao L, Lv B, Ma X, Xu N, Xia X, Deng X, Zheng C, Huang K (2017)
878 Building a multipurpose insertional mutant library for forward and reverse genetics in
879 *Chlamydomonas*. *Plant Methods* 13:36. doi:10.1186/s13007-017-0183-5
- 880 Chu VT, Weber T, Wefers B, Wurst W, Sander S, Rajewsky K, Kuhn R (2015) Increasing the
881 efficiency of homology-directed repair for CRISPR-Cas9-induced precise gene editing in
882 mammalian cells. *Nat Biotechnol* 33 (5):543-548. doi:10.1038/nbt.3198

- 883 Cong L, Ran FA, Cox D, Lin S, Barreto R, Habib N, Hsu PD, Wu X, Jiang W, Marraffini LA,
884 Zhang F (2013) Multiplex genome engineering using CRISPR/Cas systems. *Science* (New
885 York, N Y) 339 (6121):819-823
- 886 Deisseroth K, Hegemann P (2017) The form and function of channelrhodopsin. *Science* 357
887 (6356). doi:10.1126/science.aan5544
- 888 Doench JG, Hartenian E, Graham DB, Tothova Z, Hegde M, Smith I, Sullender M, Ebert BL,
889 Xavier RJ, Root DE (2014) Rational design of highly active sgRNAs for CRISPR-Cas9-
890 mediated gene inactivation. *Nat Biotechnol* 32 (12):1262-U1130. doi:10.1038/nbt.3026
- 891 Engel BD, Schaffer M, Kuhn Cuellar L, Villa E, Plitzko JM, Baumeister W (2015) Native
892 architecture of the Chlamydomonas chloroplast revealed by in situ cryo-electron
893 tomography. *Elife* 4. doi:10.7554/elife.04889
- 894 Fuhrmann M, Oertel W, Hegemann P (1999) A synthetic gene coding for the green fluorescent
895 protein (GFP) is a versatile reporter in Chlamydomonas reinhardtii. *Plant Journal* 19
896 (3):353-361
- 897 Gagnon JA, Valen E, Thyme SB, Huang P, Akhmetova L, Pauli A, Montague TG, Zimmerman S,
898 Richter C, Schier AF (2014) Efficient mutagenesis by Cas9 protein-mediated
899 oligonucleotide insertion and large-scale assessment of single-guide RNAs. *PLoS One* 9
900 (5):e98186. doi:10.1371/journal.pone.0098186
- 901 Galvan A, Gonzalez-Ballester D, Fernandez E (2007) Insertional mutagenesis as a tool to study
902 genes/functions in Chlamydomonas. *Adv Exp Med Biol* 616:77-89
- 903 Geissmann Q (2013) OpenCFU, a new free and open-source software to count cell colonies and
904 other circular objects. *PLoS One* 8 (2):e54072. doi:10.1371/journal.pone.0054072
- 905 Gillham NW, Boynton JE, Johnson AM, Burkhardt BD (1987) Mating type linked mutations
906 which disrupt the uniparental transmission of chloroplast genes in chlamydomonas.
907 *Genetics* 115 (4):677-684
- 908 Gorman DS, Levine RP (1965) Cytochrome f and plastocyanin: their sequence in the
909 photosynthetic electron transport chain of Chlamydomonas reinhardi. *Proceedings of the*
910 *National Academy of Sciences of the United States of America* 54 (6):1665-1669
- 911 Govorunova EG, Jung KH, Sineshchekov OA, Spudich JL (2004) Chlamydomonas sensory
912 Rhodopsins A and B: Cellular content and role in photophobic responses. *Biophys J* 86
913 (4):2342-2349
- 914 Guo J, Gaj T, Barbas CF, 3rd (2010) Directed evolution of an enhanced and highly efficient FokI
915 cleavage domain for zinc finger nucleases. *Journal of molecular biology* 400 (1):96-107
- 916 Harz H, Nonnengasser C, Hegemann P (1992) The Photoreceptor Current of the Green-Alga
917 Chlamydomonas. *Philosophical Transactions of the Royal Society of London Series B-*
918 *Biological Sciences* 338 (1283):39-52
- 919 Hegemann P, Bruck B (1989) Light-Induced Stop Response in Chlamydomonas-Reinhardtii -
920 Occurrence and Adaptation Phenomena. *Cell Motility and the Cytoskeleton* 14 (4):501-
921 515
- 922 Holland EM, Braun FJ, Nonnengasser C, Harz H, Hegemann P (1996) Nature of rhodopsin-
923 triggered photocurrents in Chlamydomonas .1. Kinetics and influence of divalent ions.
924 *Biophys J* 70 (2):924-931
- 925 Huang KY, Beck CF (2003) Photoropin is the blue-light receptor that controls multiple steps in
926 the sexual life cycle of the green alga Chlamydomonas reinhardtii. *Proceedings of the*
927 *National Academy of Sciences of the United States of America* 100 (10):6269-6274

- 928 Inwood W, Yoshihara C, Zalpuri R, Kim KS, Kustu S (2008) The ultrastructure of a
929 Chlamydomonas reinhardtii mutant strain lacking phytoene synthase resembles that of a
930 colorless alga. Mol Plant 1 (6):925-937. doi:10.1093/mp/ssn046
- 931 Jakab G, Mougin A, Kis M, Pollak T, Antal M, Branolant C, Solymosy F (1997) Chlamydomonas
932 U2, U4 and U6 snRNAs. An evolutionary conserved putative third interaction between U4
933 and U6 snRNAs which has a counterpart in the U4atac-U6atac snRNA duplex. Biochimie
934 79 (7):387-395
- 935 Jiang W, Brueggeman AJ, Horken KM, Plucinak TM, Weeks DP (2014) Successful transient
936 expression of Cas9 and single guide RNA genes in *Chlamydomonas reinhardtii*.
937 Eukaryotic cell 13 (11):1465-1469. doi:10.1128/EC.00213-14
- 938 Jiang W, Zhou H, Bi H, Fromm M, Yang B, Weeks DP (2013) Demonstration of
939 CRISPR/Cas9/sgRNA-mediated targeted gene modification in Arabidopsis, tobacco,
940 sorghum and rice. Nucleic acids research 41 (20):e188. doi:10.1093/nar/gkt780
- 941 Jiang WZ, Dumm S, Knuth ME, Sanders SL, Weeks DP (2017) Precise oligonucleotide-directed
942 mutagenesis of the *Chlamydomonas reinhardtii* genome. Plant Cell Rep 36 (6):1001-1004.
943 doi:10.1007/s00299-017-2138-8
- 944 Jiang WZ, Weeks DP (2017) A gene-within-a-gene Cas9/sgRNA hybrid construct enables gene
945 editing and gene replacement strategies in *Chlamydomonas reinhardtii*. Algal research in
946 press. doi:doi.org/10.1016/j.algal.2017.04.001
- 947 Jinek M, Chylinski K, Fonfara I, Hauer M, Doudna JA, Charpentier E (2012) A programmable
948 dual-RNA-guided DNA endonuclease in adaptive bacterial immunity. Science 337
949 (6096):816-821. doi:10.1126/science.1225829
- 950 Jinek M, East A, Cheng A, Lin S, Ma E, Doudna J (2013) RNA-programmed genome editing in
951 human cells. eLife 2:e00471. doi:10.7554/eLife.00471
- 952 Kao PH, Ng IS (2017) CRISPRi mediated phosphoenolpyruvate carboxylase regulation to
953 enhance the production of lipid in *Chlamydomonas reinhardtii*. Bioresour Technol.
954 doi:10.1016/j.biortech.2017.04.111
- 955 Kateriya S, Nagel G, Bamberg E, Hegemann P (2004) "Vision" in single-celled algae. News in
956 Physiological Sciences 19:133-137
- 957 Kim S, Kim D, Cho SW, Kim J, Kim JS (2014) Highly efficient RNA-guided genome editing in
958 human cells via delivery of purified Cas9 ribonucleoproteins. Genome Res 24 (6):1012-
959 1019. doi:10.1101/gr.171322.113
- 960 Kindle KL (1990) High-frequency nuclear transformation of *Chlamydomonas reinhardtii*.
961 Proceedings of the National Academy of Sciences of the United States of America 87
962 (3):1228-1232
- 963 Kirst H, Garcia-Cerdan JG, Zurbriggen A, Ruehle T, Melis A (2012) Truncated photosystem
964 chlorophyll antenna size in the green microalga *Chlamydomonas reinhardtii* upon deletion
965 of the TLA3-CpSRP43 gene. Plant physiology 160 (4):2251-2260.
966 doi:10.1104/pp.112.206672
- 967 Kouranova E, Forbes K, Zhao G, Warren J, Bartels A, Wu Y, Cui X (2016) CRISPRs for Optimal
968 Targeting: Delivery of CRISPR Components as DNA, RNA, and Protein into Cultured
969 Cells and Single-Cell Embryos. Hum Gene Ther 27 (6):464-475.
970 doi:10.1089/hum.2016.009
- 971 Li X, Zhang R, Patena W, Gang SS, Blum SR, Ivanova N, Yue R, Robertson JM, Lefebvre PA,
972 Fitz-Gibbon ST, Grossman AR, Jonikas MC (2016) An Indexed, Mapped Mutant Library

- 973 Enables Reverse Genetics Studies of Biological Processes in Chlamydomonas reinhardtii.
974 The Plant cell 28 (2):367-387
- 975 Liang X, Potter J, Kumar S, Ravinder N, Chesnut JD (2017) Enhanced CRISPR/Cas9-mediated
976 precise genome editing by improved design and delivery of gRNA, Cas9 nuclease, and
977 donor DNA. J Biotechnol 241:136-146. doi:10.1016/j.jbiotec.2016.11.011
- 978 Luck M, Hegemann P (2017) The two parallel Photocycles of the Chlamydomonas Sensory
979 Photoreceptor Histidine Kinase Rhodopsin 1. J Plant Phys 217:77-84. doi:
980 10.1016/j.jplph.2017.07.008.
- 981 Luck M, Mathes T, Bruun S, Fudim R, Hagedorn R, Tran Nguyen TM, Kateriya S, Kennis JT,
982 Hildebrandt P, Hegemann P (2012) A photochromic histidine kinase rhodopsin (HKR1)
983 that is bimodally switched by ultraviolet and blue light. The Journal of biological
984 chemistry 287 (47):40083-40090. doi:10.1074/jbc.M112.401604
- 985 Mali P, Yang L, Esvelt KM, Aach J, Guell M, DiCarlo JE, Norville JE, Church GM (2013) RNA-
986 guided human genome engineering via Cas9. Science (New York, N Y) 339 (6121):823-
987 826
- 988 McCarthy SS, Kobayashi MC, Niyogi KK (2004) White mutants of Chlamydomonas reinhardtii
989 are defective in phytoene synthase. Genetics 168 (3):1249-1257
- 990 Meinecke L, Alawady A, Schröda M, Willows R, Kobayashi MC, Niyogi KK, Grimm B, Beck
991 CF (2010) Chlorophyll-deficient mutants of Chlamydomonas reinhardtii that accumulate
992 magnesium protoporphyrin IX. Plant Mol Biol 72 (6):643-658. doi:10.1007/s11103-010-
993 9604-9
- 994 Miller JC, Holmes MC, Wang J, Guschin DY, Lee YL, Rupniewski I, Beausejour CM, Waite AJ,
995 Wang NS, Kim KA, Gregory PD, Pabo CO, Rebar EJ (2007) An improved zinc-finger
996 nuclease architecture for highly specific genome editing. Nat Biotechnol 25 (7):778-785.
997 doi:10.1038/nbt1319
- 998 Mittelmeier TM, Boyd JS, Lamb MR, Dieckmann CL (2011) Asymmetric properties of the
999 Chlamydomonas reinhardtii cytoskeleton direct rhodopsin photoreceptor localization. The
1000 Journal of cell biology 193 (4):741-753. doi:10.1083/jcb.201009131
- 1001 Mittelmeier TM, Thompson MD, Ozturk E, Dieckmann CL (2013) Independent localization of
1002 plasma membrane and chloroplast components during eyespot assembly. Eukaryotic cell
1003 12 (9):1258-1270. doi:10.1128/EC.00111-13
- 1004 Muller N, Wenzel S, Zou Y, Kunzel S, Sasso S, Weiss D, Prager K, Grossman A, Kottke T,
1005 Mittag M (2017) A Plant Cryptochrome Controls Key Features of the Chlamydomonas
1006 Circadian Clock and Its Life Cycle. Plant physiology 174 (1):185-201.
1007 doi:10.1104/pp.17.00349
- 1008 Nagel G, Ollig D, Fuhrmann M, Kateriya S, Mustl AM, Bamberg E, Hegemann P (2002)
1009 Channelrhodopsin-1: A light-gated proton channel in green algae. Science 296
1010 (5577):2395-2398
- 1011 Nagel G, Szellas T, Huhn W, Kateriya S, Adeishvili N, Berthold P, Ollig D, Hegemann P,
1012 Bamberg E (2003) Channelrhodopsin-2, a directly light-gated cation-selective membrane
1013 channel. Proceedings of the National Academy of Sciences of the United States of
1014 America 100 (24):13940-13945
- 1015 Penzkofer A, Luck M, Mathes T, Hegemann P (2014) Bistable retinal schiff base photodynamics
1016 of histidine kinase rhodopsin HKR1 from Chlamydomonas reinhardtii. Photochemistry
1017 and photobiology 90 (4):773-785. doi:10.1111/php.12246

- 1018 Petroutsos D, Tokutsu R, Maruyama S, Flori S, Greiner A, Magneschi L, Cusant L, Kottke T,
1019 Mittag M, Hegemann P, Finazzi G, Minagawa J (2016) A blue-light photoreceptor
1020 mediates the feedback regulation of photosynthesis. *Nature* 537 (7621):563-566.
1021 doi:10.1038/nature19358
- 1022 Ran FA, Cong L, Yan WX, Scott DA, Gootenberg JS, Kriz AJ, Zetsche B, Shalem O, Wu X,
1023 Makarova KS, Koonin EV, Sharp PA, Zhang F (2015) In vivo genome editing using
1024 *Staphylococcus aureus* Cas9. *Nature* 520 (7546):186-191
- 1025 Ran FA, Hsu PD, Wright J, Agarwala V, Scott DA, Zhang F (2013) Genome engineering using
1026 the CRISPR-Cas9 system. *Nat Protoc* 8 (11):2281-2308. doi:10.1038/nprot.2013.143
- 1027 Roberts DGW, Lamb MR, Dieckmann CL (2001) Characterization of the EYE2 gene required for
1028 eyespot assembly in *Chlamydomonas reinhardtii*. *Genetics* 158 (3):1037-1049
- 1029 Sander JD, Zaback P, Joung JK, Voytas DF, Dobbs D (2007) Zinc Finger Targeter (ZiFiT): an
1030 engineered zinc finger/target site design tool. *Nucleic acids research* 35 (Web Server
1031 issue):W599-605. doi:10.1093/nar/gkm349
- 1032 Schneider F, Grimm C, Hegemann P (2015) Biophysics of channelrhodopsin. *Ann Rev Biophys*
1033 44:167 – 186 doi:10.1146/annurev-biophys-060414-034014
- 1034 Schröda M, Blocker D, Beck CF (2000) The HSP70A promoter as a tool for the improved
1035 expression of transgenes in *Chlamydomonas*. *The Plant journal : for cell and molecular
1036 biology* 21 (2):121-131
- 1037 Shalem O, Sanjana NE, Hartenian E, Shi X, Scott DA, Mikkelsen T, Heckl D, Ebert BL, Root
1038 DE, Doench JG, Zhang F (2014) Genome-scale CRISPR-Cas9 knockout screening in
1039 human cells. *Science* 343 (6166):84-87. doi:10.1126/science.1247005
- 1040 Shin SE, Lim JM, Koh HG, Kim EK, Kang NK, Jeon S, Kwon S, Shin WS, Lee B, Hwangbo K,
1041 Kim J, Ye SH, Yun JY, Seo H, Oh HM, Kim KJ, Kim JS, Jeong WJ, Chang YK, Jeong
1042 BR (2016) CRISPR/Cas9-induced knockout and knock-in mutations in *Chlamydomonas
1043 reinhardtii*. *Scientific reports* 6:27810. doi:10.1038/srep27810
- 1044 Sineshchekov OA, Jung KH, Spudich JL (2002) Two rhodopsins mediate phototaxis to low- and
1045 high-intensity light in *Chlamydomonas reinhardtii*. *Proceedings of the National Academy
1046 of Sciences of the United States of America* 99 (13):8689-8694
- 1047 Sizova I, Fuhrmann M, Hegemann P (2001) A *Streptomyces rimosus* *aphVIII* gene coding for a
1048 new type phosphotransferase provides stable antibiotic resistance to *Chlamydomonas
1049 reinhardtii*. *Gene* 277 (1-2):221-229
- 1050 Sizova I, Greiner A, Awasthi M, Kateriya S, Hegemann P (2013) Nuclear gene targeting in
1051 *Chlamydomonas* using engineered zinc-finger nucleases. *The Plant journal : for cell and
1052 molecular biology* 73 (5):873-882. doi:10.1111/tpj.12066
- 1053 Spexard M, Thoing C, Beel B, Mittag M, Kottke T (2014) Response of the Sensory animal-like
1054 cryptochrome aCRY to blue and red light as revealed by infrared difference spectroscopy.
1055 *Biochemistry* 53 (6):1041-1050. doi:10.1021/bi401599z
- 1056 Sternberg SH, Redding S, Jinek M, Greene EC, Doudna JA (2014) DNA interrogation by the
1057 CRISPR RNA-guided endonuclease Cas9. *Nature* 507 (7490):62-67.
1058 doi:10.1038/nature13011
- 1059 Trippens J, Greiner A, Schellwat J, Neukam M, Rottmann T, Lu YH, Kateriya S, Hegemann P,
1060 Kreimer G (2012) Phototropin Influence on Eyespot Development and Regulation of
1061 Phototactic Behavior in *Chlamydomonas reinhardtii*. *Plant Cell* 24 (11):4687-4702.
1062 doi:Doi 10.1105/Tpc.112.103523

1063 Uhl R, Hegemann P (1990) Probing Visual Transduction in a Plant-Cell - Optical-Recording of
1064 Rhodopsin-Induced Structural-Changes from Chlamydomonas-Reinhardtii. Biophys J 58
1065 (5):1295-1302
1066 Umen JG, Goodenough UW (2001) Control of cell division by a retinoblastoma protein homolog
1067 in Chlamydomonas. Genes Dev 15 (13):1652-1661. doi:10.1101/gad.892101
1068 Yamano T, Iguchi H, Fukuzawa H (2013) Rapid transformation of Chlamydomonas reinhardtii
1069 without cell-wall removal. J Biosci Bioeng 115 (6):691-694.
1070 doi:10.1016/j.jbiosc.2012.12.020
1071 Zheng X, Yang S, Zhang D, Zhong Z, Tang X, Deng K, Zhou J, Qi Y, Zhang Y (2016) Effective
1072 screen of CRISPR/Cas9-induced mutants in rice by single-strand conformation
1073 polymorphism. Plant Cell Rep 35 (7):1545-1554. doi:10.1007/s00299-016-1967-1
1074 Zhu C, Bortesi L, Baysal C, Twyman RM, Fischer R, Capell T, Schillberg S, Christou P (2017)
1075 Characteristics of Genome Editing Mutations in Cereal Crops. Trends Plant Sci 22 (1):38-
1076 52. doi:10.1016/j.tplants.2016.08.009
1077 Zorin B, Hegemann P, Sizova I (2005) Nuclear-gene targeting by using single-stranded DNA
1078 avoids illegitimate DNA integration in Chlamydomonas reinhardtii. Eukaryotic cell 4
1079 (7):1264-1272. doi:10.1128/EC.4.7.1264-1272.2005
1080 Zorin B, Lu Y, Sizova I, Hegemann P (2009) Nuclear gene targeting in Chlamydomonas as
1081 exemplified by disruption of the PHOT gene. Gene 432 (1-2):91-96.
1082 doi:10.1016/j.gene.2008.11.028
1083 Zou Y, Wenzel S, Muller N, Prager K, Jung EM, Kothe E, Kottke T, Mittag M (2017) An
1084 Animal-Like Cryptochrome Controls the Chlamydomonas Sexual Cycle. Plant physiology
1085 174 (3):1334-1347. doi:10.1104/pp.17.00493
1086
1087

1088 **Figure Legends**

1089 **Figure 1. *Chlamydomonas* Photoreceptors**

1090 Overview of *Chlamydomonas reinhardtii* photoreceptors and domain structure. Gene IDs taken
1091 from Phytozome V12. AA indicates the number of amino acids.

1092
1093 **Figure 2. Optimization of zinc finger nuclease (ZFNs) and transformation parameters**

1094 (A) Schematic drawing of a gene targeting selection (GTS) construct. Transcription of the GTS
1095 cassette is controlled by the HSP70A/RBCS2 promoter and PSAD-Terminator. *ble* (phleomycin
1096 resistance gene) was used as a selection marker to isolate the GTS strains; the nuclease target site
1097 for any GOI (gene of interest) can be inserted into mut-*aphVIII* [GOI][*ChR1*]. *ChR1*-ZFNs serve
1098 as a control to test the HDR (homology directed repair) capabilities of GTS strains. *eyfp*:
1099 enhanced yellow fluorescent protein gene; GS₅: Glycine-Serine linker; *aphVIII*: paromomycin
1100 resistance marker; pHDR-APHVIII^{Δ120}: HDR plasmid to restore *aphVIII* functionality.

1101 (B) ZFN target site sequences inserted into mut-*aphVIII* (pGTS1-3) used to create the GTS-
1102 strains. The *ChR1*-ZFN target sequence served as a control in all pGTS plasmids. pGTS1 includes
1103 the ChR2-a-ZFN target site and pGTS2 includes the respective ChR2-b-ZFN target site. pGTS3
1104 includes the target site from the human *EMX1* homeobox protein gene and was created to test the
1105 HDR capability of Cas9. Binding sites of left and right ZF-domains for *ChR1*, *ChR2*-a, and *ChR2*-
1106 b are underlined. Binding site of *EMX1* gRNA is underlined. Protospacer adjacent motif (PAM) is
1107 highlighted in grey.

1108 (C) Workflow for the generation of a GTS strain followed by HDR experiments. Electroporation-
1109 1: pGTS-[1-3] is electroporated into a *C. reinhardtii* strain. Single colonies are isolated on
1110 Zeocin™ containing agar plates. Next, isolated and synchronously cultured GTS strains are
1111 concentrated and heat shocked before Electroporation 2. Here, functional nucleases (plasmid-
1112 encoded or recombinant) may induce the formation of DNA-DSBs within their respective mut-
1113 *aphVIII* target site and trigger HDR with co-applied donor DNA, which results in selectable
1114 paromomycin resistant (PmR) cells. After electroporation and before paromomycin selection, the
1115 cells are allowed to recover for 24 hours at 22°C or 33°C.

1116 (D) GTS-strain experiments. Bars indicate the number of PmR colonies per transformation
1117 reaction. Secondary Y-axis: selection frequencies (PmR colonies / 4x10⁶ electroporated cells).
1118 *FokI*-domain variants (mutations are indicated) were tested in their efficiency to introduce DNA-
1119 DSBs, thereby promoting HDR of mut-*aphVIII* in 3403-GTS1. Controls without heat shock
1120 before transformation (w/o HS) or without ZFN plasmids (w/o ZFN). Middle: Functionality of
1121 *ChR2*-ZFNs was tested in GTS-strain 3403-GTS2. The same results were obtained in the CC-503
1122 background (503-GTS2). Right: *ChR1*-ZFNs (3403-GTS3) in combination with different HDR
1123 donors as indicated and recovery temperatures of 22°C and 33°C. Error bars indicate standard
1124 deviation and white circles reflect individual data points.

1125 (E) Sequence alignment of amplified mut-*aphVIII* [*EMX1*][*ChR1*] (3403-GTS1) and repaired
1126 *aphVIII* loci from PmR colonies after HDR. Hyphens indicate deleted nucleotides. A point
1127 mutation found in one clone from (C) iii is indicated in red.

1128

1129 **Figure 3. Inactivation of non-selectable genes using zinc-finger nucleases**

1130 (A) Schematic diagram of *ChR1* (*COP3*) with exons shown as blue rectangles and the ZFN target
1131 site shown in yellow. HDR donors *ChR1*:FLAG and *ChR1*:mCherry are illustrated. Homology

1132 regions are identical for both constructs, and sequence insertions are centered on the ZFN
1133 cleavage site. For the FLAG insert, two stop codons were added in-frame at the 3'end, whereas
1134 mCherry was inserted in-frame without stop codons.

1135 (B) 78 amino acids at the C-terminus of ChR1:FLAG are missing due to the presence of stop
1136 codons after FLAG. The mCherry coding sequence is integrated in-frame.

1137 (C) Generation of *chr1* and *chr2* mutants in strain CC-3403. Cells were transformed via
1138 electroporation of ChR1- or ChR2-ZFN plasmids, and HDR donors as indicated. The ChR2-
1139 FLAG donor plasmid was constructed in a manner analogous to that of ChR1:FLAG, as shown in
1140 Figure 3A. The *chr1* disruption strain was transformed again to obtain the *chr1 chr2* double
1141 disruption strains. Bars reflect the number of HDR events found for 96 colonies analyzed.
1142 Conditions for ChR2-b-ZFNs were replicated. Error bar shows triplicates \pm s.d.

1143 (D) Sequencing results of *chr1* [1-8] and *chr2* [1-18] target locus amplicons. *chr1* [8] and *chr2*
1144 [16] contain additional sequences from the HDR-donor plasmid. The clones *chr2* [17, 18] were
1145 generated without HDR donors, resulting in small InDels (NHEJ; +23, -8 bp) at the cleavage site.

1146 (E) Protein immunoblotting of Channelrhodopsin-1 mutants (*chr1*) using anti-ChR1 antiserum
1147 and secondary HRP-conjugated antibody for chemiluminescence detection. M: marker. Ponceau
1148 staining was used as a loading control.

1149 (F) Protein immunoblotting of Channelrhodopsin-2 mutants (*chr2*) using anti-ChR2 antiserum
1150 and secondary HRP-conjugated antibody for chemiluminescence detection. Total ChR2
1151 abundance in CC-3403 is low (*chr1* background). ChR2 depletion is visible in *chr1 chr2* double
1152 knockouts. Ponceau staining was used as a loading control. The protein below the co-migrating
1153 ChR1 and ChR2 proteins is labeled unspecifically and is not encoded by *ChR1* or *ChR2*.

1154

1155 **Figure 4. Physiological analysis of ChR1 and ChR2 disruption strains**

1156 (A) Light-scattering assay of strains as indicated. Phototactic responses to different intensities of
1157 blue light (455 nm). 100% light corresponds to 1.25×10^{21} photons $m^{-2} s^{-1}$. Numbers below
1158 correspond to the various light intensities employed.

1159 (B) Phototactic sensitivity of various *Chlamydomonas* lines. Initial linear slopes of the light-
1160 scattering responses at 455 nm (solid lines) and 530 nm (dashed lines) were calculated ($\Delta V/\Delta s$)
1161 for CC-3403 cells and cells containing *chr1*, *chr2* or *chr1 chr2* modifications and plotted against
1162 the normalized light intensity.

1163 (C) Protein immunoblotting of two CC-3403 strains with mCherry inserted into *ChR1* (#1; #2).
1164 Anti-ChR1 antibodies detected ChR1:mCherry (~110 kDa) fusion protein. M: marker; WT: CC-
1165 3403 crude extracts; Ponceau staining was used as a loading control.
1166 (D) Confocal microscopy: Live cell imaging of CC-3403 *ChR1:mCherry* strains. CC-3403 was
1167 used as a control. ChR1:mCherry is mainly located within the cell cytoplasm. Only minor
1168 fractions are found within the plasma membrane region of the eyespot (white arrow). The same
1169 settings and filters were used in all images. DIC: differential interference contrast.
1170 (E) Eyespot position. Differential contrast images of the indicated ChR1 and ChR2 disruption
1171 strains are shown at the top. Dashed line indicates equatorial position and arrowheads the eyespot.
1172 For statistical analysis, between 100 and 193 cells of each strain grown under identical conditions
1173 were analyzed.
1174 (F) Box plot (whiskers min to max) of the eyespot area of the indicated strains. ANOVA analyses
1175 with Tukey's multiple comparison post-test revealed a significant difference (**p<0.001,
1176 Supplemental Table 9) for the marked strains compared to other strains. n=62-65 cells.

1177

1178 **Figure 5. Gene disruption by genetically encoded Cas9**

1179 (A) Schematic of DNA constructs. The promoter of heat-shock protein HSP70A promotes the
1180 transcription of *Chlamydomonas* codon-adapted *S. aureus* or *S. pyogenes* Cas9. Guide RNA
1181 transcription under the control of different CrU6-promotors (#1-4). Guide sequences were
1182 inserted into vectors containing the appropriate *SaCas9* or *SpCas9* scaffold. The coding sequence
1183 of *aphVIII* (PmR) is also located on the pCrU6-plasmids to enable antibiotic selection using
1184 paromomycin. NLS: nuclear localization signal. T: poly-thymine terminator.

1185 (B) The phytoene synthase gene, *PSY1*, was chosen as a target gene. sgRNA transcription driven
1186 by *C. reinhardtii* U6 promoters (CrU6 #1-4) was assayed. Photographs of a selective agar plates
1187 from *PSY1* inactivation experiments. If the cells were allowed to recover for one day before
1188 antibiotic selection on paromomycin-containing agar plates, mixed colonies of WT and *PSY1*-
1189 inactivated mutants were obtained. If the cells were allowed to recover for two days, pure white
1190 colonies with inactivated *PSY1* were found. Recovery at 33°C for the first 24 h increased
1191 targeting frequencies for HS by approximately one third. Targeting frequencies (targeted colonies
1192 / selected colonies) are the mean of three independent experiments. HS: HSP70A promoter; HR:
1193 HSP70A/RBCS2 promoter.

1194 (C) Sequence alignment of amplified *psyI* loci from white colonies. Dots indicate spacers,
1195 hyphens indicate deleted nucleotides. “PAM” (grey) and “Protospacer” sequences are indicated.
1196 *PSYI*: wild-type gene sequence.

1197 (D) Workflow diagram summarizing steps for generation of mutants using genetically encoded
1198 Cas9. Red letters highlight the key step enabling mutant generation and isolation. The use of this
1199 two-step screening strategy (qPCR + long-range PCR) enables the isolation of clones having long
1200 insertions within the target site.

1201 (E) Genomic DNA of clones that failed in the initial qPCR locus amplification was column
1202 purified and subjected to long-range PCR (200-s elongation time). This step identified *cop5*, *chr2*,
1203 *cop1*, and *phot* mutants with target site insertions in the range of 2-5 kb. The absence of PHOT
1204 protein due to failed *phot* mutant target site amplification is shown by immunoblotting. Left:
1205 Graph summarizing the number of deletion mutants found per 96 analyzed clones. WT: target loci
1206 amplicons from CC-3403 genomic DNA.

1207 (F) *cop5* #1 and 2 amplicons from (E) were sequenced from both ends. In both cases, fragments
1208 of plasmid pCOP5-sg//PmR, used in the respective targeting experiment, had inserted into the
1209 target site by NHEJ. Hyphens indicate deleted nucleotides.

1210 (G) Integration of the full-length *SaCas9* coding sequence and sgRNA-DNA into the genomes of
1211 isolated photoreceptor mutants. WT: negative control; the pHs-*SaCas9* and pCOP5-sg//PmR
1212 plasmid templates were used as positive controls for PCR.

1213

1214 **Figure 6. Gene targeting using exogenously supplied recombinant Cas9/gRNA**
1215 **ribonucleoprotein (RNP) complexes**

1216 (A) Schematic illustrating Cas9/gRNA RNP assembly detailed in the Methods section.

1217 (B) Schematic workflow of the Cas9/gRNA RNP transformation procedure.

1218 (C) Number of PmR colonies obtained with the GTS mut-*aphVIII* repair assay from three
1219 independent transformations. Strain 3403-GTS3, with mut-*aphVIII* [*EMX1*] and [*ChR1*] target
1220 sites, was transformed with HDR-donor plasmids (pHDR-*APHVIII*^{Δ120}) and either *ChR1*-ZFN
1221 plasmids or Cas9/gRNA[*EMX1*] RNP. Selection frequency is calculated as PmR colonies /
1222 electroporated cells. The experiments were carried out as depicted in A and B except where
1223 indicated. Controls without heat shock before transformation (w/o HS).

1224 (D) Left: HDR donors contain a 30 bp target site insertion sequence (blue box, “FLAG”)
1225 surrounded by two target gene homology arms (equal length, square brackets). Right: Possible
1226 mutations and underlying repair mechanisms are drawn schematically. Arrows indicate ODN
1227 bindings sites used during PCR analysis. Colored boxes are mutation variants and refer to color-
1228 coded sequences in E-G, and squares indicate the type of modification: Dark blue: HDR on both
1229 sides, Light blue: Single side HDR detected by flag-PCR, dark grey: Single side HDR detected by
1230 locus PCR, open square: dual side NHEJ detected by locus PCR.
1231 (E-G) Left: number of identified mutants (out of 96 tested). The target site, HDR donor, and
1232 strain are indicated for each experiment. Cells were co-transformed with a selection marker
1233 (*ARG7* for CC-3403, *aphVII* for CC-125, and *aphVIII* for 3403-*uvr8*). Sequence alignment of
1234 target site amplicons from mutant strains with the corresponding *wt* sequence. Lines indicate 20
1235 bp gRNA binding sites. Predicted cutting sites are shown (▼), and NGG PAM sequences are
1236 highlighted by grey boxes. Gaps are marked with dots (.), deletions with minus signs (-). FLAG
1237 sequences are shown in blue, HDR donor sequences inserted in a non-HDR manner are shown in
1238 green, and other inserting DNA e.g., genomic DNA fragments or DNA from marker plasmids are
1239 shown in red. Premature STOP codons are underlined.
1240 (H) Protein immunoblotting using protein-specific antisera and anti-rabbit HRP-conjugated
1241 secondary antibodies for chemiluminescent visualization. Left: Immunoblotting of *cop1* mutants
1242 obtained in (E; i-iv), anti-VOP rabbit antiserum, 1:2000; middle: *uvr8* mutants described in (F),
1243 anti-UVR8 rabbit antiserum, 1:2000; right: *phot* mutants described in (G; i-iii), anti-LOV1 rabbit
1244 antiserum, 1:2000. M: marker.
1245 (I) Left: DIC images of unfixed CC-125 and CC-125 *mat3-1* cells and division clusters (upper
1246 right corner). Right: cell size distribution of CC-125 (n=167 cells), CC-125 *mat3-1* (n=170 cells)
1247 and CC-125 *mat3-2* (n=136 cells). Scale bars: 10 µm.
1248

1249 **Figure 7. Protocols for gene editing in *Chlamydomonas reinhardtii***

1250 The stepwise diagram serves as a guide for the application of ZFNs or CRISPR-Cas9 followed by
1251 mutant screening procedures. Details for every section can be found in the Methods.

1252

Overview of Chlamydomonas photoreceptors and domain structure

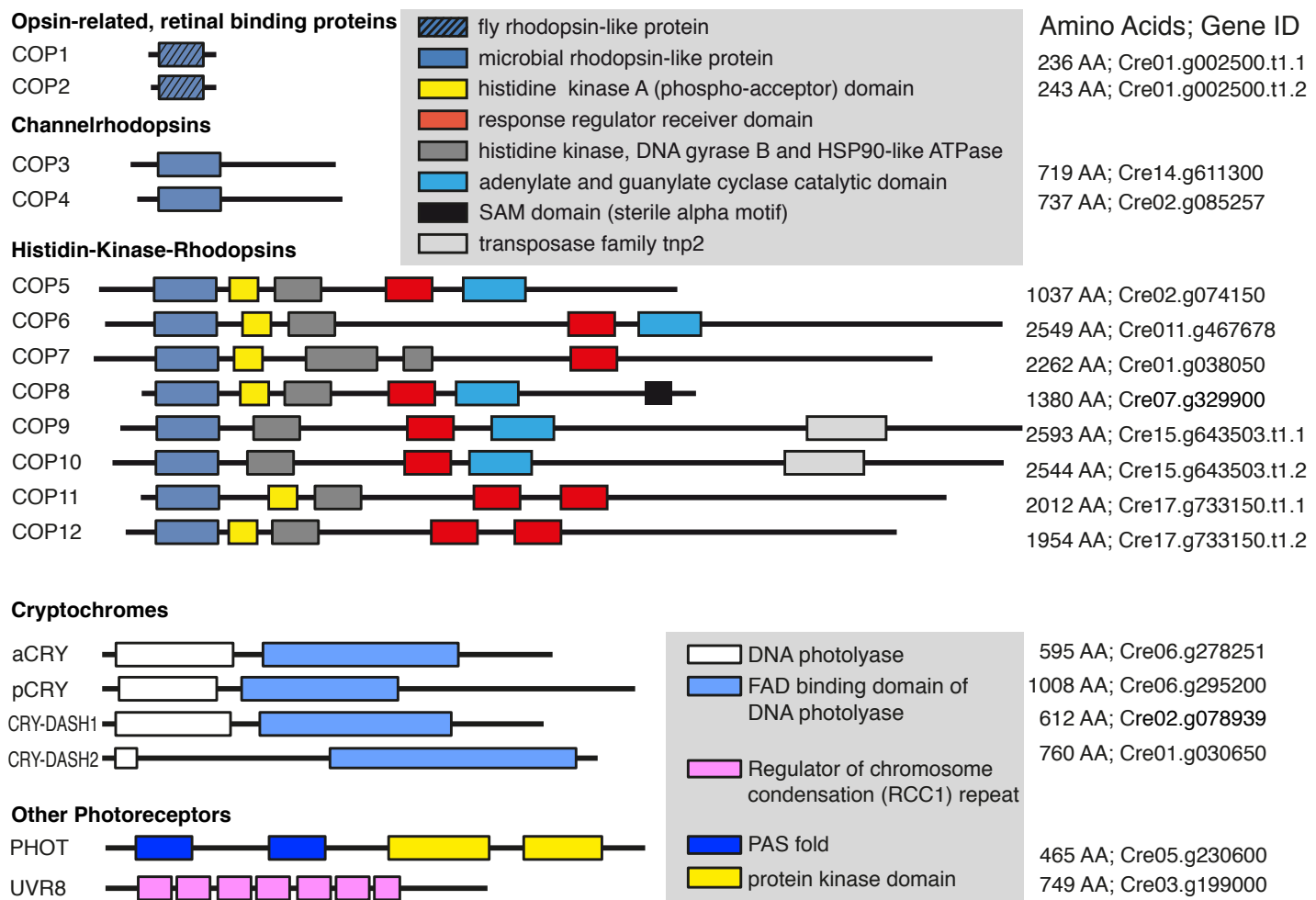
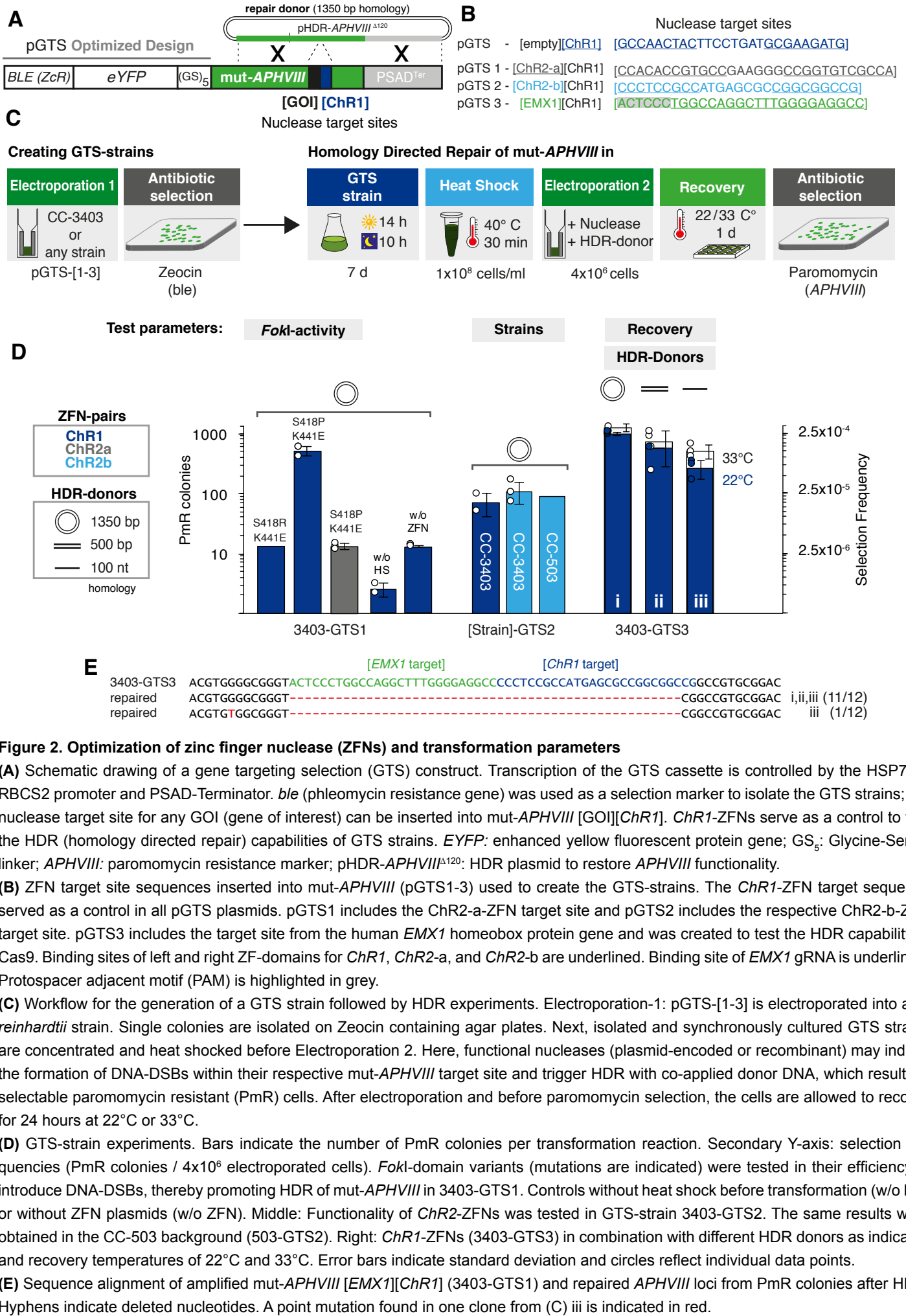


Figure 1. Chlamydomonas Photoreceptors

Overview of *Chlamydomonas reinhardtii* photoreceptors and domain structure. Gene IDs taken from Phytozome V12. AA indicates the number of amino acids.



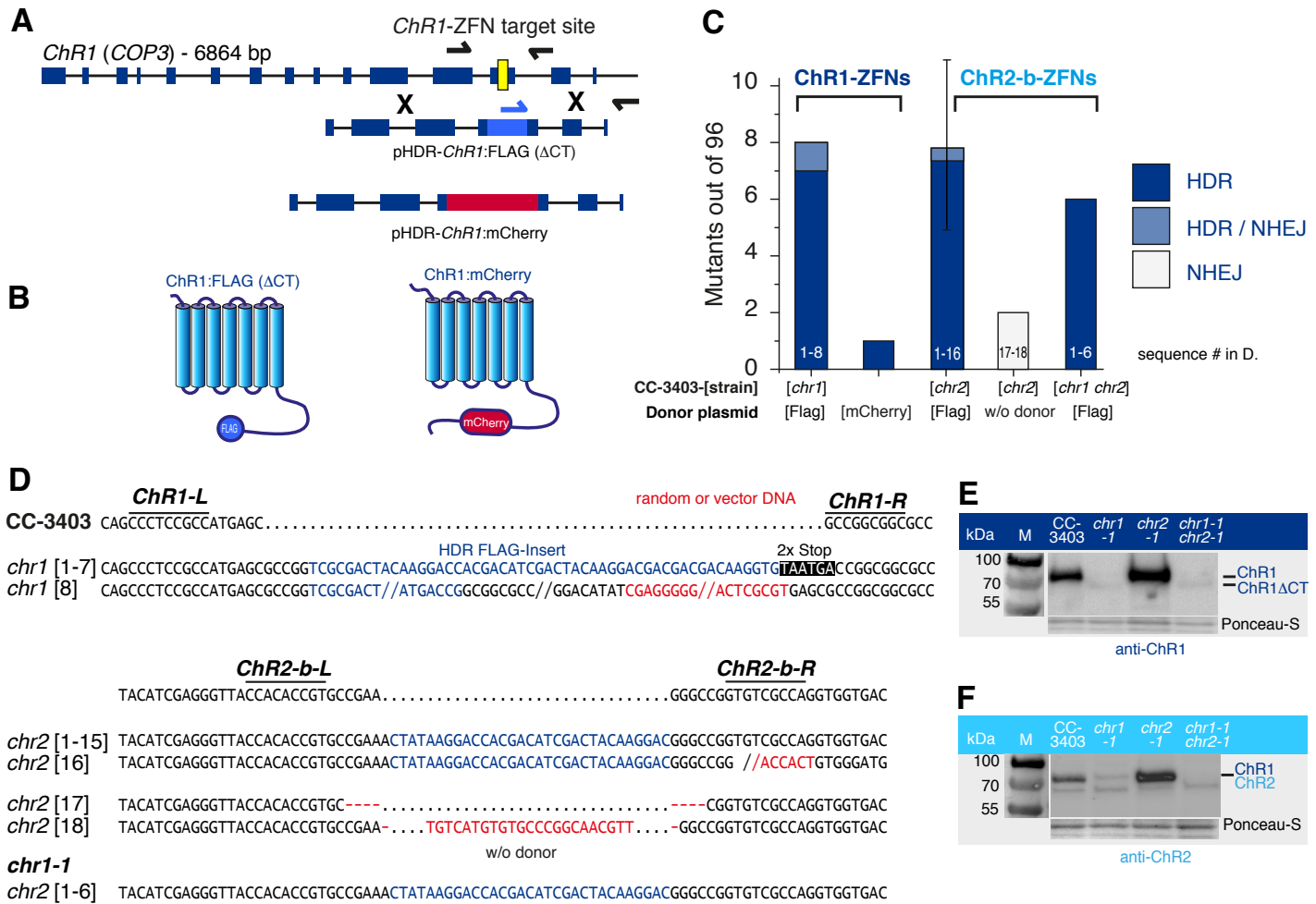


Figure 3. Inactivation of non-selectable genes using zinc-finger nucleases

(A) Schematic diagram of *ChR1* (COP3) with exons shown as blue rectangles and the ZFN target site shown in yellow. HDR donors ChR1:FLAG and ChR1:mCherry are illustrated. Homology regions are identical for both constructs, and sequence insertions are centered on the ZFN cleavage site. For the FLAG insert, two stop codons were added in-frame at the 3' end, whereas mCherry was inserted in-frame without stop codons.

(B) 78 amino acids at the C-terminus of ChR1:FLAG are missing due to the presence of stop codons after FLAG. The mCherry coding sequence is integrated in-frame.

(C) Generation of *chr1* and *chr2* mutants in strain CC-3403. Cells were transformed via electroporation of ChR1- or ChR2-ZFN plasmids, and HDR donors as indicated. The ChR2-FLAG donor plasmid was constructed in a manner analogous to that of ChR1:FLAG, as shown in Figure 3A. The *chr1* disruption strain was transformed again to obtain the *chr1 chr2* double disruption strains. Bars reflect the number of HDR events found for 96 colonies analyzed. Conditions for ChR2-b-ZFNs were replicated. Error bar shows triplicates \pm s.d.

(D) Sequencing results of *chr1* [1-8] and *chr2* [1-18] target locus amplicons. *chr1* [8] and *chr2* [16] contain additional sequences from the HDR-donor plasmid. The clones *chr2* [17, 18] were generated without HDR donors, resulting in small InDels (NHEJ; +23, -8 bp) at the cleavage site.

(E) Protein immunoblotting of Channelrhodopsin-1 mutants (*chr1*) using anti-ChR1 antiserum and secondary HRP-conjugated antibody for chemiluminescence detection. M: marker. Ponceau staining was used as a loading control.

(F) Protein immunoblotting of Channelrhodopsin-2 mutants (*chr2*) using anti-ChR2 antiserum and secondary HRP-conjugated antibody for chemiluminescence detection. Total ChR2 abundance in CC-3403 is low (*chr1* background). ChR2 depletion is visible in *chr1 chr2* double knockouts. Ponceau staining was used as a loading control. The protein below the co-migrating ChR1 and ChR2 proteins is labeled unspecifically and is not encoded by *ChR1* or *ChR2*.

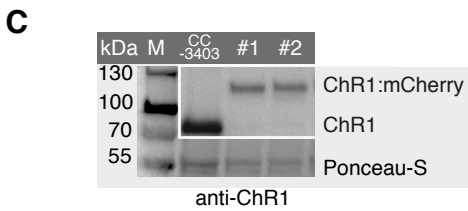
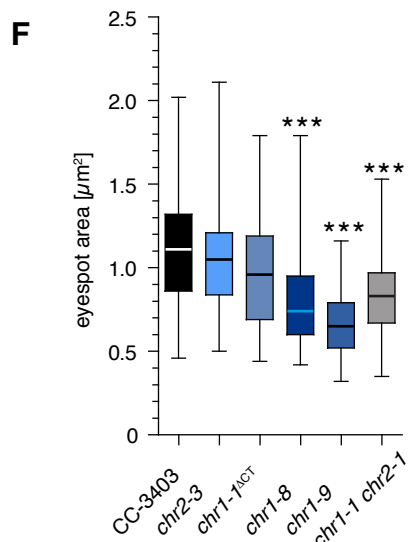
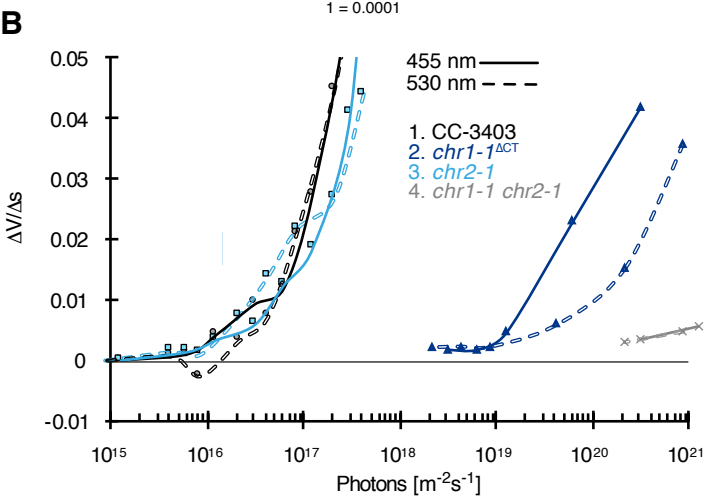
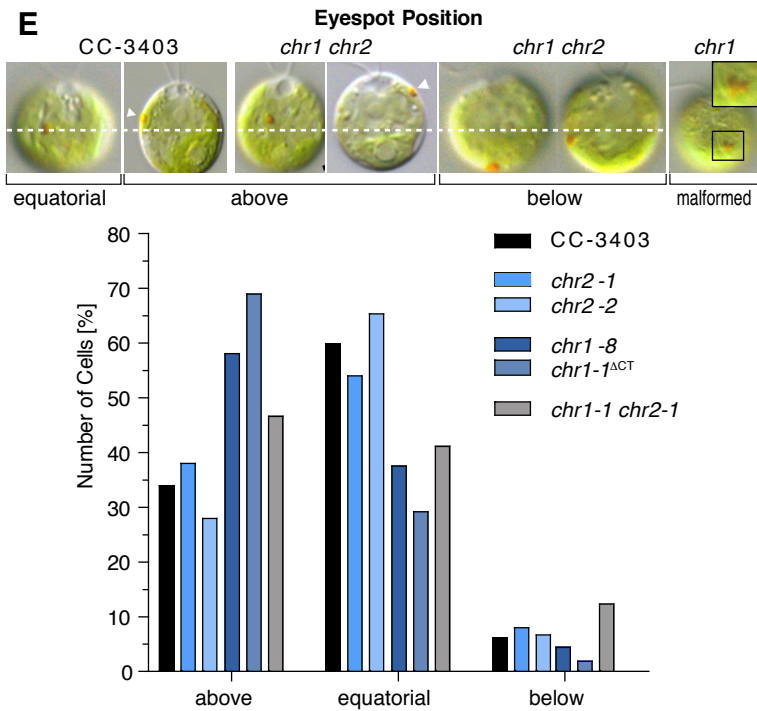
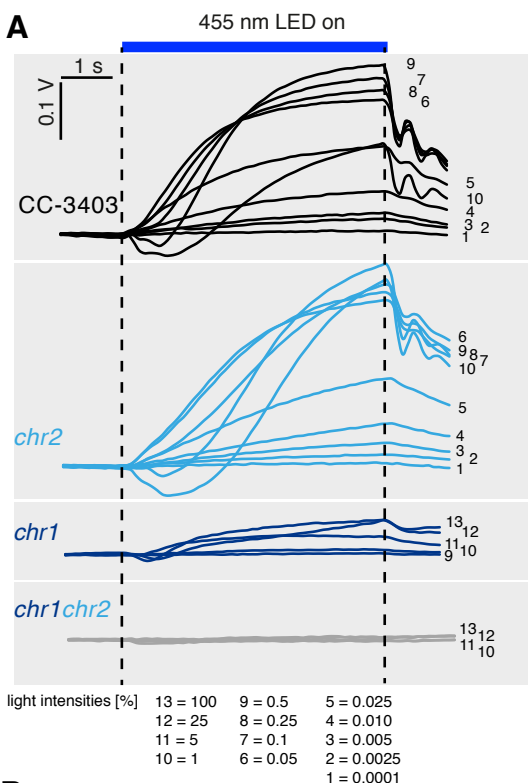


Figure 4. Physiological analysis of ChR1 and ChR2 disruption strains

(A) Light-scattering assay of strains as indicated. Phototactic responses to different intensities of blue light (455 nm). 100% light corresponds to 1.25×10^{21} photons $m^{-2} s^{-1}$. Numbers below correspond to the various light intensities employed.

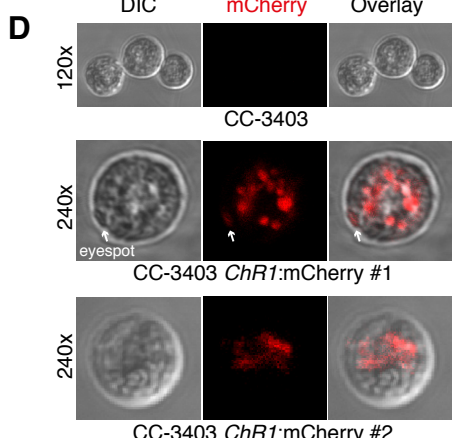
(B) Phototactic sensitivity of various *Chlamydomonas* lines. Initial linear slopes of the light-scattering responses at 455 nm (solid lines) and 530 nm (dashed lines) were calculated ($\Delta V/\Delta s$) for CC-3403 cells and cells containing *chr1*, *chr2* or *chr1 chr2* modifications and plotted against the normalized light intensity.

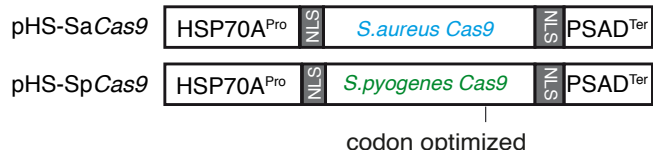
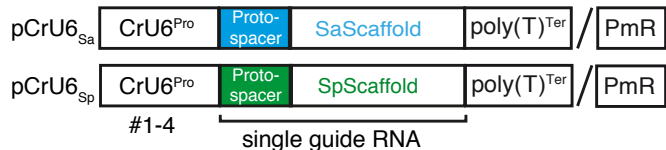
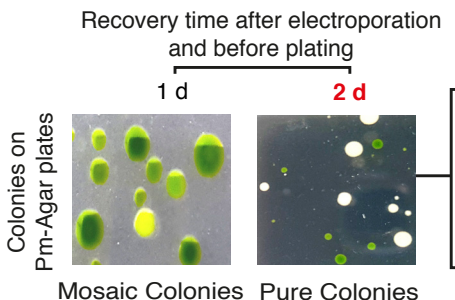
(C) Protein immunoblotting of two CC-3403 strains with mCherry inserted into *ChR1* (#1; #2). Anti-ChR1 antibodies detected ChR1:mCherry (~110 kDa) fusion protein. M: marker; WT: CC-3403 crude extracts; Ponceau staining was used as a loading control.

(D) Confocal microscopy: Live cell imaging of CC-3403 *ChR1:mCherry* strains. CC-3403 was used as a control. ChR1:mCherry is mainly located within the cell cytoplasm. Only minor fractions are found within the plasma membrane region of the eyespot (white arrow). The same settings and filters were used in all images. DIC: differential interference contrast.

(E) Eyespot position. Differential contrast images of the indicated ChR1 and ChR2 disruption strains are shown at the top. Dashed line indicates equatorial position and arrowheads the eyespot. For statistical analysis, between 100 and 193 cells of each strain grown under identical conditions were analyzed.

(F) Box plot (whiskers min to max) of the eyespot area of the indicated strains. ANOVA analyses with Tukey's multiple comparison post-test revealed a significant difference (**p<0.001, Supplemental Table 9) for the marked strains compared to other strains. n=62-65 cells.



A**Cas9 expression constructs****sgRNA transcription constructs****B****PSY1 deletion experiments in CC-3403****PSY1 Targeting frequency**

	SpCas9	SaCas9
Promoter	HS	
CrU6-#1	-	0.006
CrU6-#2	0.010	0.009
CrU6-#3	0.033	-
CrU6-#4	-	0.089 0.160 0.024

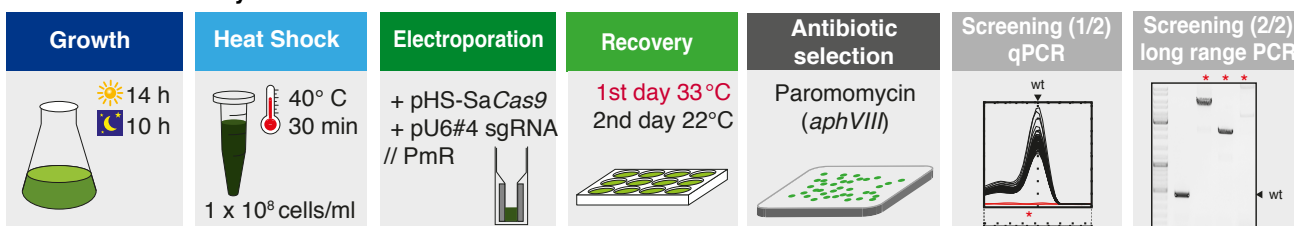
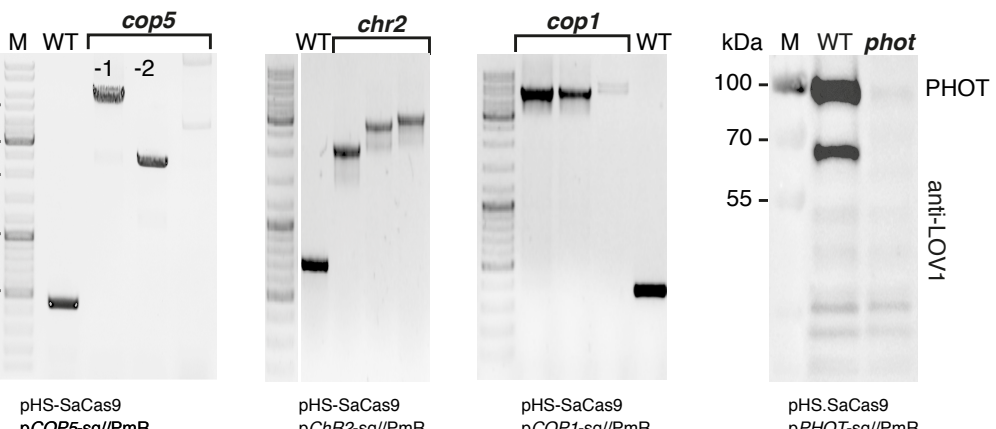
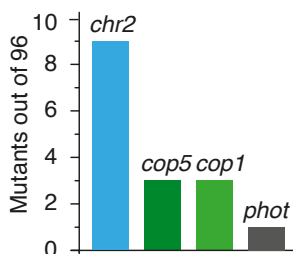
Recovery 1st day at 22°C 1st day at 33°C
2nd day at 22°C 2nd day at 22°C

PSY1

C**Protospacer****CC-3403 *psy1* sequence alignments**

TCGCCACGAGGCTTCAAGTGGAG.....
TGCCACGAGGCTTCAAGTGGGA.....
TGCCACGAGGCTTCAAGT-----
TGCCACGAGGCTTCAAGTGGAG.....
TGCCACGAGGCTTCAAGTGGAGGTTTTAAATCAATCTAAAGTATATAAGTAAACTTGGTCTGACAGTTACCAATGCCGGGGAGTGGTGTGACAGGGTACGAGAAATG (1/96)
TGCCACGAGGCTTCAAGTGGAGGTTTTAAATCAATCTAAAGTATATAAGTAAACTTGGTCTGACAGTTACCAATGCCGGGGAGTGGTGTGACAGGGTACGAGAAATG (1/96)

parts of pHS-SaCas9 backbone

D Workflow: Genetically encoded Cas9**E****CC-3403 mutants****F****CC-3403 cop5 sequence alignments**

COP5 CACATGCAGTCGACCCCTCGCAATGGCACATCAATCACACTGCAGGTGACTCGGTGATGCTGGCGACGTGCTGATGATCACATTCCGCTTCTGGCTTCTGGCTACAAACAAAGGTATGTCAGTGGATTAC
cop5-1 CACATGCAGTCGACCCCTCGCAATGGCACATCAATCACACTGCAGGTGACTCGGTGATGCTGGCGACGTGCTGATGATCACATTCCGCTTCTGGCTTCTGGCTACAA---[+ 5.1 KB]---TAC
cop5-2 CAC---[+ 2.0 KB]---CCAGTGAGTTAC

Protospacer PAM

fragments of pCOP5-sg//PmR

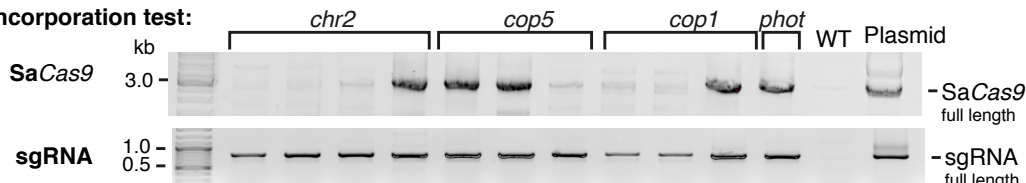
G**Genomic incorporation test:**

Figure 5. Gene disruption by genetically encoded Cas9

(A) Schematic of DNA constructs. The promoter of heat-shock protein HSP70A promotes the transcription of *Chlamydomonas* codon-adapted *S. aureus* or *S. pyogenes* Cas9. Guide RNA transcription under the control of different CrU6-promotors (#1-4). Guide sequences were inserted into vectors containing the appropriate SaCas9 or SpCas9 scaffold. The coding sequence of APHVIII (PmR) is also located on the pCrU6-plasmids to enable antibiotic selection using paromomycin. NLS: nuclear localization signal. T: poly-thymine terminator.

(B) The phytoene synthase gene, *PSY1*, was chosen as a target gene. sgRNA transcription driven by *C. reinhardtii* U6 promoters (CrU6 #1-4) was assayed. Photographs of a selective agar plates from *PSY1* inactivation experiments. If the cells were allowed to recover for one day before antibiotic selection on paromomycin-containing agar plates, mixed colonies of WT and *PSY1*-inactivated mutants were obtained. If the cells were allowed to recover for two days, pure white colonies with inactivated *PSY1* were found. Recovery at 33°C for the first 24 h increased targeting frequencies for HS by approximately one third. Targeting frequencies (targeted colonies / selected colonies) are the mean of three independent experiments. HS: HSP70A promoter; HR: HSP70A/RBCS2 promoter.

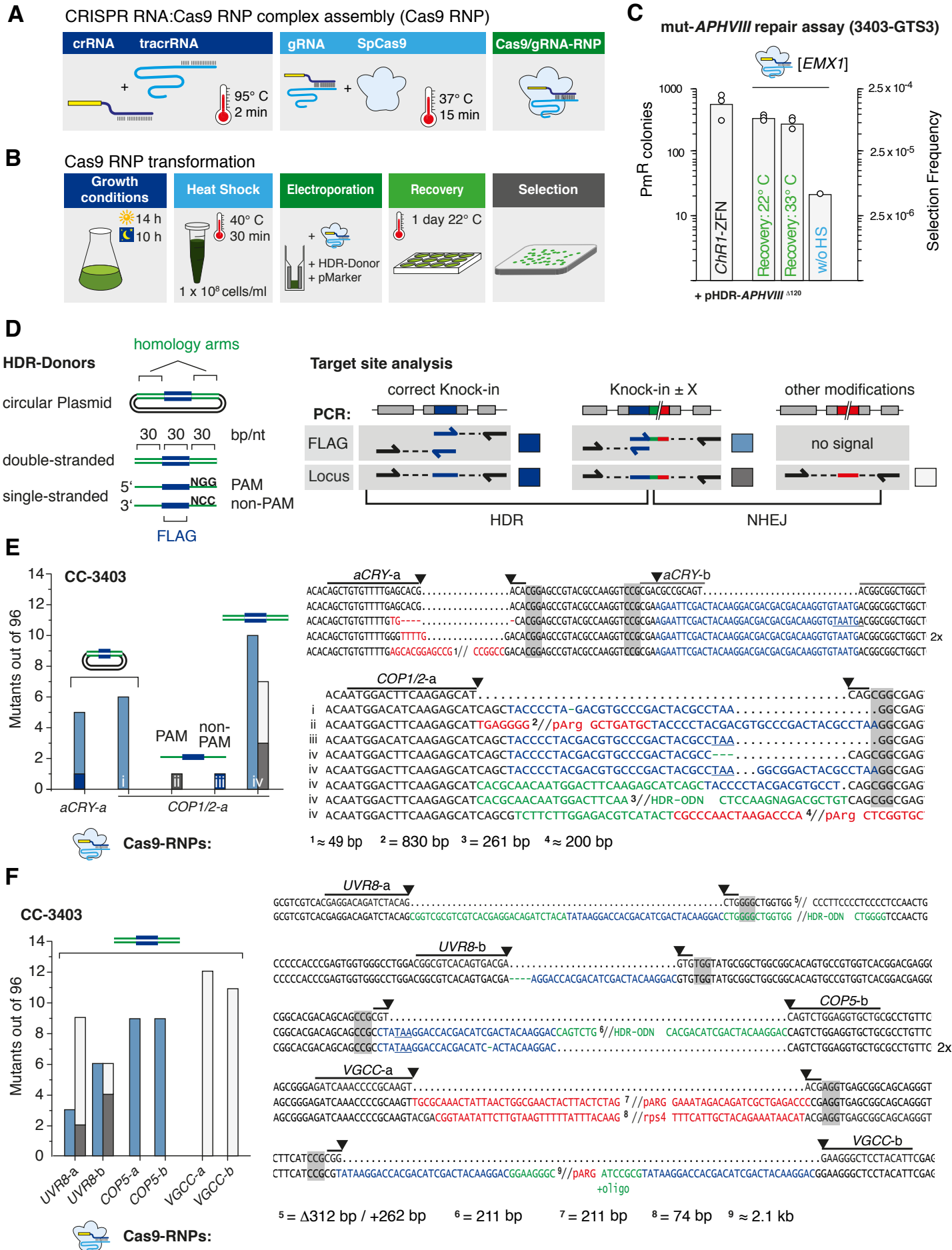
(C) Sequence alignment of amplified *psy1* loci from white colonies. Dots indicate spacers, hyphens indicate deleted nucleotides. "PAM" (grey) and "Protospacer" sequences are indicated. *PSY1*: wild-type gene sequence.

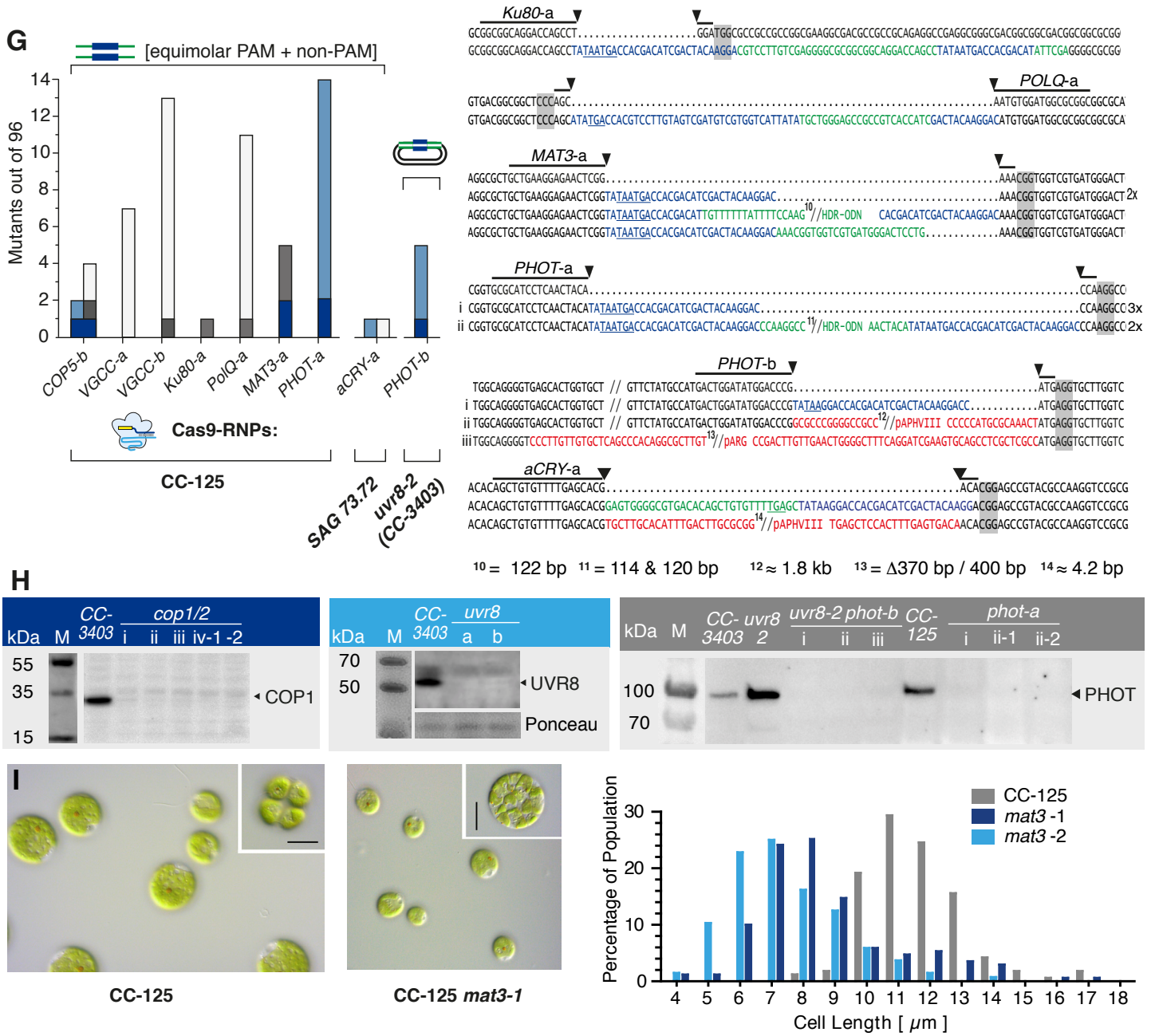
(D) Workflow diagram summarizing steps for generation of mutants using genetically encoded Cas9. Red letters highlight the key step enabling mutant generation and isolation. The use of this two-step screening strategy (qPCR + long-range PCR) enables the isolation of clones having long insertions within the target site.

(E) Genomic DNA of clones that failed in the initial qPCR locus amplification was column purified and subjected to long-range PCR (200-s elongation time). This step identified *cop5*, *chr2*, *cop1*, and *phot* mutants with target site insertions in the range of 2-5 kb. The absence of PHOT protein due to failed *phot* mutant target site amplification is shown by immunoblotting. Left: Graph summarizing the number of deletion mutants found per 96 analyzed clones. WT: target loci amplicons from CC-3403 genomic DNA.

(F) *cop5* #1 and 2 amplicons from (E) were sequenced from both ends. In both cases, fragments of plasmid pCOP5-sg//PmR, used in the respective targeting experiment, had inserted into the target site by NHEJ. Hyphens indicate deleted nucleotides.

(G) Integration of the full-length SaCas9 coding sequence and sgRNA-DNA into the genomes of isolated photoreceptor mutants. WT: negative control; the pHS-SaCas9 and pCOP5-sg//PmR plasmid templates were used as positive controls for PCR.





vFigure 6. Gene targeting using exogenously supplied recombinant Cas9/gRNA ribonucleoprotein (RNP) complexes

(A) Schematic illustrating Cas9/gRNA RNP assembly detailed in the Methods section.

(B) Schematic workflow of the Cas9/gRNA RNP transformation procedure.

(C) Number of PmR colonies obtained with the GTS mut-*APHVIII* repair assay from three independent transformations. Strain 3403-GTS3, with mut-*APHVIII* [*EMX1*] and [*ChR1*] target sites, was transformed with HDR-donor plasmids (pHDR-*APHVIII*¹²⁰) and either *ChR1*-ZFN plasmids or Cas9/gRNA[*EMX1*] RNP. Selection frequency is calculated as PmR colonies / electroporated cells. The experiments were carried out as depicted in A and B except where indicated. Controls without heat shock before transformation (w/o HS).

(D) Left: HDR donors contain a 30 bp target site insertion sequence (blue box, "FLAG") surrounded by two target gene homology arms (equal length, square brackets). Right: Possible mutations and underlying repair mechanisms are drawn schematically. Arrows indicate ODN binding sites used during PCR analysis. Colored boxes are mutation variants and refer to color-coded sequences in E-G, and squares indicate the type of modification: Dark blue: HDR on both sides, Light blue: Single side HDR detected by flag-PCR, dark grey: Single side HDR detected by locus PCR, open square: dual side NHEJ detected by locus PCR.

(E-G) Left: number of identified mutants (out of 96 tested). The target site, HDR donor, and strain are indicated for each experiment. Cells were co-transformed with a selection marker (*ARG7* for CC-3403, *APHVII* for CC-125, and *APHVIII* for 3403-*uvr8*). Sequence alignment of target site amplicons from mutant strains with the corresponding *wt* sequence. Lines indicate 20 bp gRNA binding sites. Predicted cutting sites are shown (\blacktriangledown), and NGG PAM sequences are highlighted by grey boxes. Gaps are marked with dots (.), deletions with minus signs (-). FLAG sequences are shown in blue, HDR donor sequences inserted in a non-HDR manner are shown in green, and other inserting DNA e.g., genomic DNA fragments or DNA from marker plasmids are shown in red. Premature STOP codons are underlined.

(H) Protein immunoblotting using protein-specific antisera and anti-rabbit HRP-conjugated secondary antibodies for chemiluminescent visualization. Left: Immunoblotting of *cop1* mutants obtained in (E; i-iv), anti-VOP rabbit antiserum, 1:2000; middle: *uvr8* mutants described in (F), anti-UVR8 rabbit antiserum, 1:2000; right: *phot* mutants described in (G; i-iii), anti-LOV1 rabbit antiserum, 1:2000. M: marker.

(I) Left: DIC images of unfixed CC-125 and CC-125 *mat3-1* cells and division clusters (upper right corner). Right: cell size distribution of CC-125 (n=167 cells), CC-125 *mat3-1* (n=170 cells) and CC-125 *mat3-2* (n=136 cells). Scale bars: 10 μ m.

Methods Section			A) ZFN plasmid	B) Cas9 plasmid	C) Cas9/gRNA RNP	Time scale			
#1	Culturing	Strain:	CC-3403, CC-503	CC-3403	CC-3403, CC-125, SAG73.72	1 week	Day 1-7		
			- Growth: TAP(±Arg), 110 rpm, synchronized: 14 h light 25 °C - 10 h dark 18°C - logarithmic growth for >1 week						
#2	Prepare DNA + protein	- see Methods				1 week			
#3	<i>C. reinhardtii</i> /transformation	3.1 Heat-Shock Buffer:	- Harvest cells at 1-3x10 ⁶ cells/ml, concentrate to 1x10 ⁸ cells/ml - Incubate at 40°C for 30 min at 350 rpm			4 h	Day 8		
			TAP-sucrose 40 mM	TAP-sucrose 40 mM	ME-sucrose 40 mM				
		3.2 Nucleases	- 1 µg pZFN-L - 1 µg pZFN-R	- 2 µg pCas9 plasmid - 1 µg sgRNA plasmid	- 10 pmol RNP complex (1.6 µg Cas9 protein, 10 pmol tracr:crRNA)				
		3.3 HDR Donors	Donor sequences contain a 30 bp FLAG insert with STOP codon: - Oligonucleotides, 10 pmol, 90 bp, 5' 3' PTO - PCR, 500 ng, 500-1000 bp, 5' PTO - Plasmid, 2 µg, 500-1000 bp homology						
#4		3.4 Selection markers	- pH R11 (<i>ARG7</i>) - pAphVIII	<i>aphVIII</i> marker on sgRNA plasmid	- pH R11 (<i>ARG7</i>) - pAphVII - pAphVIII	4 h	Day 9-18		
		Recovery	- Transfer cells into 500 µl TAP-Arg - 24 h at 22°C or 33°C						
		Plating	- Plate on selection media pH R11: omit arginine in media pAphVII: hygromycin 10 µg/ml pAphVIII: paromomycin 10 µg/ml - Incubate for 7-10 days						
#5	Screening	Picking	- Pick clones and transfer to 180 µl TAP(±Arg) in 96 well plate			4 h	Day 19		
		Genomic DNA	5.1 Crude Extracts: - grow cells for 4 days - resuspend 40 µl cells in 20 µl dilution buffer - use 1 µl of supernatant for a 10 µl PCR reaction		5.2 Whole cell qPCR: - Use 1 µl directly for PCR without DNA isolation with qPCR Mastermix	1-2 d	Day 20-22		
		FLAG PCR	- Oligonucleotide 1: binds in GOI outside of the HDR donor sequence - Oligonucleotide 2: only binds on FLAG insert						
		Locus PCR	Short PCR on target locus reveals size differences of mutated loci: - Works best with short donors (e.g. 90 bp HDR ODNs) - Fast detection possible with high-resolution melting curve analysis on qPCR cyclers - No PCR product indicates integration of long inserts			1 d	Day 23		
Sequencing	Locus PCR with long elongation - if possible: send for sequencing - if not (Integration of long inserts): perform protein immunoblot analysis								
	Isolate mutant	- choose positive mutants from 96 well plate and isolate homogenous clone (dilute, plate, pick) - confirm analysis							

Figure 7. Protocols for gene editing in *Chlamydomonas reinhardtii*

The stepwise diagram serves as a guide for the application of ZFNs or CRISPR-Cas9 followed by mutant screening procedures. Details for every section can be found in the Methods.

Parsed Citations

Bæk K, Kim DH, Jeong J, Sim SJ, Melis A, Kim JS, Jin E, Bae S (2016) DNA-free two-gene knockout in *Chlamydomonas reinhardtii* via CRISPR-Cas9 ribonucleoproteins. *Scientific reports* 6:30620. doi:10.1038/srep30620

Pubmed: [Author and Title](#)

CrossRef: [Author and Title](#)

Google Scholar: [Author Only Title Only Author and Title](#)

Beel B, Prager K, Spexard M, Sasso S, Weiss D, Muller N, Heinrichs M, Dewez D, Ikoma D, Grossman AR, Kottke T, Mittag M (2012) A flavin binding cryptochromes photoreceptor responds to both blue and red light in *Chlamydomonas reinhardtii*. *Plant Cell* 24 (7):2992-3008. doi:10.1105/tpc.112.098947

Pubmed: [Author and Title](#)

CrossRef: [Author and Title](#)

Google Scholar: [Author Only Title Only Author and Title](#)

Berthold P, Schmitt R, Mages W (2002) An engineered *Streptomyces hygroscopicus* aph 7" gene mediates dominant resistance against hygromycin B in *Chlamydomonas reinhardtii*. *Protist* 153 (4):401-412. doi:10.1078/14344610260450136

Pubmed: [Author and Title](#)

CrossRef: [Author and Title](#)

Google Scholar: [Author Only Title Only Author and Title](#)

Berthold P, Tsunoda SP, Ernst OP, Mages W, Gradmann D, Hegemann P (2008) Channelrhodopsin-1 initiates phototaxis and photophobic responses in *Chlamydomonas* by immediate light-induced depolarization. *Plant Cell* 20 (6):1665-1677. doi:10.1105/tpc.108.057919

Pubmed: [Author and Title](#)

CrossRef: [Author and Title](#)

Google Scholar: [Author Only Title Only Author and Title](#)

Bibikova M, Beumer K, Trautman JK, Carroll D (2003) Enhancing gene targeting with designed zinc finger nucleases. *Science* 300 (5620):764. doi:10.1126/science.1079512

Pubmed: [Author and Title](#)

CrossRef: [Author and Title](#)

Google Scholar: [Author Only Title Only Author and Title](#)

Boyd JS, Mittelmeier TM, Dieckmann CL (2011a) New insights into eyespot placement and assembly in *Chlamydomonas*. *BioArchitecture* 1:196-199. doi:10.4161/bioa.1.4.17697

Pubmed: [Author and Title](#)

CrossRef: [Author and Title](#)

Google Scholar: [Author Only Title Only Author and Title](#)

Boyd JS, Mittelmeier TM, Lamb MR, Dieckmann CL (2011b) Thioredoxin-family protein EYE2 and Ser/Thr kinase EYE3 play interdependent roles in eyespot assembly. *Mol Biol Cell* 22 (9):1421-1429. doi:10.1091/mbc.E10-11-0918

Pubmed: [Author and Title](#)

CrossRef: [Author and Title](#)

Google Scholar: [Author Only Title Only Author and Title](#)

Braun FJ, Hegemann P (1999) Two light-activated conductances in the eye of the green alga *Volvox carteri*. *Biophys J* 76 (3):1668-1678

Pubmed: [Author and Title](#)

CrossRef: [Author and Title](#)

Google Scholar: [Author Only Title Only Author and Title](#)

Ceccaldi R, Rondinelli B, D'Andrea AD (2016) Repair Pathway Choices and Consequences at the Double-Strand Break. *Trends Cell Biol* 26 (1):52-64. doi:10.1016/j.tcb.2015.07.009

Pubmed: [Author and Title](#)

CrossRef: [Author and Title](#)

Google Scholar: [Author Only Title Only Author and Title](#)

Cheng X, Liu G, Ke W, Zhao L, Lv B, Ma X, Xu N, Xia X, Deng X, Zheng C, Huang K (2017) Building a multipurpose insertional mutant library for forward and reverse genetics in *Chlamydomonas*. *Plant Methods* 13:36. doi:10.1186/s13007-017-0183-5

Pubmed: [Author and Title](#)

CrossRef: [Author and Title](#)

Google Scholar: [Author Only Title Only Author and Title](#)

Chu VT, Weber T, Wefers B, Wurst W, Sander S, Rajewsky K, Kuhn R (2015) Increasing the efficiency of homology-directed repair for CRISPR-Cas9-induced precise gene editing in mammalian cells. *Nat Biotechnol* 33 (5):543-548. doi:10.1038/nbt.3198

Pubmed: [Author and Title](#)

CrossRef: [Author and Title](#)

Google Scholar: [Author Only Title Only Author and Title](#)

Cong L, Ran FA, Cox D, Lin S, Barretto R, Habib N, Hsu PD, Wu X, Jiang W, Marraffini LA, Zhang F (2013) Multiplex genome engineering using CRISPR/Cas systems. *Science (New York, N Y)* 339 (6121):819-823

Pubmed: [Author and Title](#)

CrossRef: [Author and Title](#)

Google Scholar: [Author Only Title Only Author and Title](#)

Deisseroth K, Hegemann P (2017) The form and function of channelrhodopsin. *Science* 357 (6356). doi:10.1126/science.aan5544

Pubmed: [Author and Title](#)

CrossRef: [Author and Title](#)

Google Scholar: [Author Only](#) [Title Only](#) [Author and Title](#)

Doench JG, Hartenian E, Graham DB, Tothova Z, Hegde M, Smith I, Sullender M, Ebert BL, Xavier RJ, Root DE (2014) Rational design of highly active sgRNAs for CRISPR-Cas9-mediated gene inactivation. *Nat Biotechnol* 32 (12):1262-U1130. doi:10.1038/nbt.3026

Pubmed: [Author and Title](#)

CrossRef: [Author and Title](#)

Google Scholar: [Author Only](#) [Title Only](#) [Author and Title](#)

Engel BD, Schaffer M, Kuhn Cuellar L, Villa E, Plitzko JM, Baumeister W (2015) Native architecture of the Chlamydomonas chloroplast revealed by *in situ* cryo-electron tomography. *eLife* 4. doi:10.7554/eLife.04889

Pubmed: [Author and Title](#)

CrossRef: [Author and Title](#)

Google Scholar: [Author Only](#) [Title Only](#) [Author and Title](#)

Fuhrmann M, Oertel W, Hegemann P (1999) A synthetic gene coding for the green fluorescent protein (GFP) is a versatile reporter in *Chlamydomonas reinhardtii*. *Plant Journal* 19 (3):353-361

Pubmed: [Author and Title](#)

CrossRef: [Author and Title](#)

Google Scholar: [Author Only](#) [Title Only](#) [Author and Title](#)

Gagnon JA, Valen E, Thyme SB, Huang P, Akhmetova L, Pauli A, Montague TG, Zimmerman S, Richter C, Schier AF (2014) Efficient mutagenesis by Cas9 protein-mediated oligonucleotide insertion and large-scale assessment of single-guide RNAs. *PLoS One* 9 (5):e98186. doi:10.1371/journal.pone.0098186

Pubmed: [Author and Title](#)

CrossRef: [Author and Title](#)

Google Scholar: [Author Only](#) [Title Only](#) [Author and Title](#)

Galvan A, Gonzalez-Ballester D, Fernandez E (2007) Insertional mutagenesis as a tool to study genes/functions in Chlamydomonas. *Adv Exp Med Biol* 616:77-89

Pubmed: [Author and Title](#)

CrossRef: [Author and Title](#)

Google Scholar: [Author Only](#) [Title Only](#) [Author and Title](#)

Geissmann Q (2013) OpenCFU, a new free and open-source software to count cell colonies and other circular objects. *PLoS One* 8 (2):e54072. doi:10.1371/journal.pone.0054072

Pubmed: [Author and Title](#)

CrossRef: [Author and Title](#)

Google Scholar: [Author Only](#) [Title Only](#) [Author and Title](#)

Gillham NW, Boynton JE, Johnson AM, Burkhardt BD (1987) Mating type linked mutations which disrupt the uniparental transmission of chloroplast genes in chlamydomonas. *Genetics* 115 (4):677-684

Pubmed: [Author and Title](#)

CrossRef: [Author and Title](#)

Google Scholar: [Author Only](#) [Title Only](#) [Author and Title](#)

Gorman DS, Levine RP (1965) Cytochrome f and plastocyanin: their sequence in the photosynthetic electron transport chain of *Chlamydomonas reinhardtii*. *Proceedings of the National Academy of Sciences of the United States of America* 54 (6):1665-1669

Pubmed: [Author and Title](#)

CrossRef: [Author and Title](#)

Google Scholar: [Author Only](#) [Title Only](#) [Author and Title](#)

Govorunova EG, Jung KH, Sineshchekov OA, Spudich JL (2004) Chlamydomonas sensory Rhodopsins A and B: Cellular content and role in photophobic responses. *Biophys J* 86 (4):2342-2349

Pubmed: [Author and Title](#)

CrossRef: [Author and Title](#)

Google Scholar: [Author Only](#) [Title Only](#) [Author and Title](#)

Guo J, Gaj T, Barbas CF, 3rd (2010) Directed evolution of an enhanced and highly efficient FokI cleavage domain for zinc finger nucleases. *Journal of molecular biology* 400 (1):96-107

Pubmed: [Author and Title](#)

CrossRef: [Author and Title](#)

Google Scholar: [Author Only](#) [Title Only](#) [Author and Title](#)

Harz H, Nonnengasser C, Hegemann P (1992) The Photoreceptor Current of the Green-Alga Chlamydomonas. *Philosophical Transactions of the Royal Society of London Series B-Biological Sciences* 338 (1283):39-52

Pubmed: [Author and Title](#)

CrossRef: [Author and Title](#)

Google Scholar: [Author Only](#) [Title Only](#) [Author and Title](#)

Hegemann P, Bruck B (1989) Light-Induced Stop Response in Chlamydomonas-Reinhardtii - Occurrence and Adaptation Phenomena. *Cell Motility and the Cytoskeleton* 14 (4):501-515

Pubmed: [Author and Title](#)

CrossRef: [Author and Title](#)

Google Scholar: [Author Only Title Only Author and Title](#)

Holland EM, Braun FJ, Nonnengasser C, Harz H, Hegemann P (1996) Nature of rhodopsin-triggered photocurrents in Chlamydomonas .1. Kinetics and influence of divalent ions. *Biophys J* 70 (2):924-931

Pubmed: [Author and Title](#)

CrossRef: [Author and Title](#)

Google Scholar: [Author Only Title Only Author and Title](#)

Huang KY, Beck CF (2003) Photoprotein is the blue-light receptor that controls multiple steps in the sexual life cycle of the green alga Chlamydomonas reinhardtii. *Proceedings of the National Academy of Sciences of the United States of America* 100 (10):6269-6274

Pubmed: [Author and Title](#)

CrossRef: [Author and Title](#)

Google Scholar: [Author Only Title Only Author and Title](#)

Inwood W, Yoshihara C, Zalpuri R, Kim KS, Kustu S (2008) The ultrastructure of a Chlamydomonas reinhardtii mutant strain lacking phytoene synthase resembles that of a colorless alga. *Mol Plant* 1 (6):925-937. doi:10.1093/mp/ssp046

Pubmed: [Author and Title](#)

CrossRef: [Author and Title](#)

Google Scholar: [Author Only Title Only Author and Title](#)

Jakab G, Mougin A, Kis M, Pollak T, Antal M, Branolant C, Solymosy F (1997) Chlamydomonas U2, U4 and U6 snRNAs. An evolutionary conserved putative third interaction between U4 and U6 snRNAs which has a counterpart in the U4atac-U6atac snRNA duplex. *Biochimie* 79 (7):387-395

Pubmed: [Author and Title](#)

CrossRef: [Author and Title](#)

Google Scholar: [Author Only Title Only Author and Title](#)

Jiang W, Brueggeman AJ, Horken KM, Plucinak TM, Weeks DP (2014) Successful transient expression of Cas9 and single guide RNA genes in Chlamydomonas reinhardtii. *Eukaryotic cell* 13 (11):1465-1469. doi:10.1128/EC.00213-14

Pubmed: [Author and Title](#)

CrossRef: [Author and Title](#)

Google Scholar: [Author Only Title Only Author and Title](#)

Jiang W, Zhou H, Bi H, Fromm M, Yang B, Weeks DP (2013) Demonstration of CRISPR/Cas9/sgRNA-mediated targeted gene modification in Arabidopsis, tobacco, sorghum and rice. *Nucleic acids research* 41 (20):e188. doi:10.1093/nar/gkt780

Pubmed: [Author and Title](#)

CrossRef: [Author and Title](#)

Google Scholar: [Author Only Title Only Author and Title](#)

Jiang WZ, Dumm S, Knuth ME, Sanders SL, Weeks DP (2017) Precise oligonucleotide-directed mutagenesis of the Chlamydomonas reinhardtii genome. *Plant Cell Rep* 36 (6):1001-1004. doi:10.1007/s00299-017-2138-8

Pubmed: [Author and Title](#)

CrossRef: [Author and Title](#)

Google Scholar: [Author Only Title Only Author and Title](#)

Jiang WZ, Weeks DP (2017) A gene-within-a-gene Cas9/sgRNA hybrid construct enables gene editing and gene replacement strategies in Chlamydomonas reinhardtii. *Algal research* in press. doi:doi.org/10.1016/j.algal.2017.04.001

Pubmed: [Author and Title](#)

CrossRef: [Author and Title](#)

Google Scholar: [Author Only Title Only Author and Title](#)

Jinek M, Chylinski K, Fonfara I, Hauer M, Doudna JA, Charpentier E (2012) A programmable dual-RNA-guided DNA endonuclease in adaptive bacterial immunity. *Science* 337 (6096):816-821. doi:10.1126/science.1225829

Pubmed: [Author and Title](#)

CrossRef: [Author and Title](#)

Google Scholar: [Author Only Title Only Author and Title](#)

Jinek M, East A, Cheng A, Lin S, Ma E, Doudna J (2013) RNA-programmed genome editing in human cells. *eLife* 2:e00471. doi:10.7554/eLife.00471

Pubmed: [Author and Title](#)

CrossRef: [Author and Title](#)

Google Scholar: [Author Only Title Only Author and Title](#)

Kao PH, Ng IS (2017) CRISPRi mediated phosphoenolpyruvate carboxylase regulation to enhance the production of lipid in Chlamydomonas reinhardtii. *Bioresour Technol*. doi:10.1016/j.biortech.2017.04.111

Pubmed: [Author and Title](#)

CrossRef: [Author and Title](#)

Google Scholar: [Author Only Title Only Author and Title](#)

Kateriya S, Nagel G, Bamberg E, Hegemann P (2004) "Vision" in single-celled algae. *News in Physiological Sciences* 19:133-137

Pubmed: [Author and Title](#)

CrossRef: [Author and Title](#)

Google Scholar: [Author Only Title Only Author and Title](#)

Kim S, Kim D, Cho SW, Kim J, Kim JS (2014) Highly efficient RNA-guided genome editing in human cells via delivery of purified Cas9

ribonucleoproteins. *Genome Res* 24 (6):1012-1019. doi:10.1101/gr.171322.113

Pubmed: [Author and Title](#)

CrossRef: [Author and Title](#)

Google Scholar: [Author Only Title Only Author and Title](#)

Kindle KL (1990) High-frequency nuclear transformation of *Chlamydomonas reinhardtii*. *Proceedings of the National Academy of Sciences of the United States of America* 87 (3):1228-1232

Pubmed: [Author and Title](#)

CrossRef: [Author and Title](#)

Google Scholar: [Author Only Title Only Author and Title](#)

Kirst H, Garcia-Cerdan JG, Zurbriggen A, Ruehle T, Melis A (2012) Truncated photosystem chlorophyll antenna size in the green microalga *Chlamydomonas reinhardtii* upon deletion of the TLA3-CpSRP43 gene. *Plant physiology* 160 (4):2251-2260. doi:10.1104/pp.112.206672

Pubmed: [Author and Title](#)

CrossRef: [Author and Title](#)

Google Scholar: [Author Only Title Only Author and Title](#)

Kouranova E, Forbes K, Zhao G, Warren J, Bartels A, Wu Y, Cui X (2016) CRISPRs for Optimal Targeting: Delivery of CRISPR Components as DNA, RNA, and Protein into Cultured Cells and Single-Cell Embryos. *Hum Gene Ther* 27 (6):464-475. doi:10.1089/hum.2016.009

Pubmed: [Author and Title](#)

CrossRef: [Author and Title](#)

Google Scholar: [Author Only Title Only Author and Title](#)

Li X, Zhang R, Patena W, Gang SS, Blum SR, Ivanova N, Yue R, Robertson JM, Lefebvre PA, Fitz-Gibbon ST, Grossman AR, Jonikas MC (2016) An Indexed, Mapped Mutant Library Enables Reverse Genetics Studies of Biological Processes in *Chlamydomonas reinhardtii*. *The Plant cell* 28 (2):367-387

Pubmed: [Author and Title](#)

CrossRef: [Author and Title](#)

Google Scholar: [Author Only Title Only Author and Title](#)

Liang X, Potter J, Kumar S, Ravinder N, Chesnut JD (2017) Enhanced CRISPR/Cas9-mediated precise genome editing by improved design and delivery of gRNA, Cas9 nuclease, and donor DNA. *J Biotechnol* 241:136-146. doi:10.1016/j.biote.2016.11.011

Pubmed: [Author and Title](#)

CrossRef: [Author and Title](#)

Google Scholar: [Author Only Title Only Author and Title](#)

Luck M, Hegemann P (2017) The two parallel Photocycles of the *Chlamydomonas* Sensory Photoreceptor Histidine Kinase Rhodopsin 1. *J Plant Phys* 217:77-84. doi: 10.1016/j.jplph.2017.07.008.

Pubmed: [Author and Title](#)

CrossRef: [Author and Title](#)

Google Scholar: [Author Only Title Only Author and Title](#)

Luck M, Mathes T, Bruun S, Fudim R, Hagedorn R, Tran Nguyen TM, Kateriya S, Kennis JT, Hildebrandt P, Hegemann P (2012) A photochromic histidine kinase rhodopsin (HKR1) that is bimodally switched by ultraviolet and blue light. *The Journal of biological chemistry* 287 (47):40083-40090. doi:10.1074/jbc.M112.401604

Pubmed: [Author and Title](#)

CrossRef: [Author and Title](#)

Google Scholar: [Author Only Title Only Author and Title](#)

Mali P, Yang L, Esvelt KM, Aach J, Guell M, DiCarlo JE, Norville JE, Church GM (2013) RNA-guided human genome engineering via Cas9. *Science (New York, N Y)* 339 (6121):823-826

Pubmed: [Author and Title](#)

CrossRef: [Author and Title](#)

Google Scholar: [Author Only Title Only Author and Title](#)

McCarthy SS, Kobayashi MC, Niyogi KK (2004) White mutants of *Chlamydomonas reinhardtii* are defective in phytoene synthase. *Genetics* 168 (3):1249-1257

Pubmed: [Author and Title](#)

CrossRef: [Author and Title](#)

Google Scholar: [Author Only Title Only Author and Title](#)

Meinecke L, Alawady A, Schröda M, Willows R, Kobayashi MC, Niyogi KK, Grimm B, Beck CF (2010) Chlorophyll-deficient mutants of *Chlamydomonas reinhardtii* that accumulate magnesium protoporphyrin IX. *Plant Mol Biol* 72 (6):643-658. doi:10.1007/s11103-010-9604-9

Pubmed: [Author and Title](#)

CrossRef: [Author and Title](#)

Google Scholar: [Author Only Title Only Author and Title](#)

Miller JC, Holmes MC, Wang J, Guschin DY, Lee YL, Rupniewski I, Beausejour CM, Waite AJ, Wang NS, Kim KA, Gregory PD, Pablo CO, Rebar EJ (2007) An improved zinc-finger nuclease architecture for highly specific genome editing. *Nat Biotechnol* 25 (7):778-785. doi:10.1038/nbt1319

Pubmed: [Author and Title](#)

CrossRef: [Author and Title](#)

Google Scholar: [Author Only Title Only Author and Title](#)

Mittelmeier TM, Boyd JS, Lamb MR, Dieckmann CL (2011) Asymmetric properties of the *Chlamydomonas reinhardtii* cytoskeleton direct rhodopsin photoreceptor localization. *The Journal of cell biology* 193 (4):741-753. doi:10.1083/jcb.201009131

Pubmed: [Author and Title](#)

CrossRef: [Author and Title](#)

Google Scholar: [Author Only Title Only Author and Title](#)

Mittelmeier TM, Thompson MD, Ozturk E, Dieckmann CL (2013) Independent localization of plasma membrane and chloroplast components during eyespot assembly. *Eukaryotic cell* 12 (9):1258-1270. doi:10.1128/EC.00111-13

Pubmed: [Author and Title](#)

CrossRef: [Author and Title](#)

Google Scholar: [Author Only Title Only Author and Title](#)

Muller N, Wenzel S, Zou Y, Kunzel S, Sasso S, Weiss D, Prager K, Grossman A, Kottke T, Mittag M (2017) A Plant Cryptochrome Controls Key Features of the *Chlamydomonas* Circadian Clock and Its Life Cycle. *Plant physiology* 174 (1):185-201. doi:10.1104/pp.17.00349

Pubmed: [Author and Title](#)

CrossRef: [Author and Title](#)

Google Scholar: [Author Only Title Only Author and Title](#)

Nagel G, Ollig D, Fuhrmann M, Kateriya S, Musti AM, Bamberg E, Hegemann P (2002) Channelrhodopsin-1: A light-gated proton channel in green algae. *Science* 296 (5577):2395-2398

Pubmed: [Author and Title](#)

CrossRef: [Author and Title](#)

Google Scholar: [Author Only Title Only Author and Title](#)

Nagel G, Szellas T, Huhn W, Kateriya S, Adeishvili N, Berthold P, Ollig D, Hegemann P, Bamberg E (2003) Channelrhodopsin-2, a directly light-gated cation-selective membrane channel. *Proceedings of the National Academy of Sciences of the United States of America* 100 (24):13940-13945

Pubmed: [Author and Title](#)

CrossRef: [Author and Title](#)

Google Scholar: [Author Only Title Only Author and Title](#)

Penzkofer A, Luck M, Mathes T, Hegemann P (2014) Bistable retinal schiff base photodynamics of histidine kinase rhodopsin HKR1 from *Chlamydomonas reinhardtii*. *Photochemistry and photobiology* 90 (4):773-785. doi:10.1111/php.12246

Pubmed: [Author and Title](#)

CrossRef: [Author and Title](#)

Google Scholar: [Author Only Title Only Author and Title](#)

Petrotusos D, Tokutsu R, Maruyama S, Flori S, Greiner A, Magneschi L, Cusant L, Kottke T, Mittag M, Hegemann P, Finazzi G, Minagawa J (2016) A blue-light photoreceptor mediates the feedback regulation of photosynthesis. *Nature* 537 (7621):563-566. doi:10.1038/nature19358

Pubmed: [Author and Title](#)

CrossRef: [Author and Title](#)

Google Scholar: [Author Only Title Only Author and Title](#)

Ran FA, Cong L, Yan WX, Scott DA, Gootenberg JS, Kriz AJ, Zetsche B, Shalem O, Wu X, Makarova KS, Koonin EV, Sharp PA, Zhang F (2015) In vivo genome editing using *Staphylococcus aureus* Cas9. *Nature* 520 (7546):186-191

Pubmed: [Author and Title](#)

CrossRef: [Author and Title](#)

Google Scholar: [Author Only Title Only Author and Title](#)

Ran FA, Hsu PD, Wright J, Agarwala V, Scott DA, Zhang F (2013) Genome engineering using the CRISPR-Cas9 system. *Nat Protoc* 8 (11):2281-2308. doi:10.1038/nprot.2013.143

Pubmed: [Author and Title](#)

CrossRef: [Author and Title](#)

Google Scholar: [Author Only Title Only Author and Title](#)

Roberts DGW, Lamb MR, Dieckmann CL (2001) Characterization of the EYE2 gene required for eyespot assembly in *Chlamydomonas reinhardtii*. *Genetics* 158 (3):1037-1049

Pubmed: [Author and Title](#)

CrossRef: [Author and Title](#)

Google Scholar: [Author Only Title Only Author and Title](#)

Sander JD, Zaback P, Joung JK, Voytas DF, Dobbs D (2007) Zinc Finger Targeter (ZFiT): an engineered zinc finger/target site design tool. *Nucleic acids research* 35 (Web Server issue):W599-605. doi:10.1093/nar/gkm349

Pubmed: [Author and Title](#)

CrossRef: [Author and Title](#)

Google Scholar: [Author Only Title Only Author and Title](#)

Schneider F, Grimm C, Hegemann P (2015) Biophysics of channelrhodopsin. *Ann Rev Biophys* 44:167 – 186 doi:10.1146/annurev-biophys-060414-034014

Pubmed: [Author and Title](#)

CrossRef: [Author and Title](#)

Google Scholar: [Author Only Title Only Author and Title](#)

Schroda M, Blocker D, Beck CF (2000) The HSP70A promoter as a tool for the improved expression of transgenes in Chlamydomonas. *The Plant journal : for cell and molecular biology* 21 (2):121-131

Pubmed: [Author and Title](#)

CrossRef: [Author and Title](#)

Google Scholar: [Author Only](#) [Title Only](#) [Author and Title](#)

Shalem O, Sanjana NE, Hartenian E, Shi X, Scott DA, Mikkelsen T, Heckl D, Ebert BL, Root DE, Doench JG, Zhang F (2014) Genome-scale CRISPR-Cas9 knockout screening in human cells. *Science* 343 (6166):84-87. doi:10.1126/science.1247005

Pubmed: [Author and Title](#)

CrossRef: [Author and Title](#)

Google Scholar: [Author Only](#) [Title Only](#) [Author and Title](#)

Shin SE, Lim JM, Koh HG, Kim EK, Kang NK, Jeon S, Kwon S, Shin WS, Lee B, Hwangbo K, Kim J, Ye SH, Yun JY, Seo H, Oh HM, Kim KJ, Kim JS, Jeong WJ, Chang YK, Jeong BR (2016) CRISPR/Cas9-induced knockout and knock-in mutations in Chlamydomonas reinhardtii. *Scientific reports* 6:27810. doi:10.1038/srep27810

Pubmed: [Author and Title](#)

CrossRef: [Author and Title](#)

Google Scholar: [Author Only](#) [Title Only](#) [Author and Title](#)

Sineshchekov OA, Jung KH, Spudich JL (2002) Two rhodopsins mediate phototaxis to low- and high-intensity light in Chlamydomonas reinhardtii. *Proceedings of the National Academy of Sciences of the United States of America* 99 (13):8689-8694

Pubmed: [Author and Title](#)

CrossRef: [Author and Title](#)

Google Scholar: [Author Only](#) [Title Only](#) [Author and Title](#)

Sizova I, Fuhrmann M, Hegemann P (2001) A Streptomyces rimosus aphVIII gene coding for a new type phosphotransferase provides stable antibiotic resistance to Chlamydomonas reinhardtii. *Gene* 277 (1-2):221-229

Pubmed: [Author and Title](#)

CrossRef: [Author and Title](#)

Google Scholar: [Author Only](#) [Title Only](#) [Author and Title](#)

Sizova I, Greiner A, Awasthi M, Kateriya S, Hegemann P (2013) Nuclear gene targeting in Chlamydomonas using engineered zinc-finger nucleases. *The Plant journal : for cell and molecular biology* 73 (5):873-882. doi:10.1111/tpj.12066

Pubmed: [Author and Title](#)

CrossRef: [Author and Title](#)

Google Scholar: [Author Only](#) [Title Only](#) [Author and Title](#)

Spepard M, Thoing C, Beel B, Mittag M, Kottke T (2014) Response of the Sensory animal-like cryptochrome aCRY to blue and red light as revealed by infrared difference spectroscopy. *Biochemistry* 53 (6):1041-1050. doi:10.1021/bi401599z

Pubmed: [Author and Title](#)

CrossRef: [Author and Title](#)

Google Scholar: [Author Only](#) [Title Only](#) [Author and Title](#)

Sternberg SH, Redding S, Jinek M, Greene EC, Doudna JA (2014) DNA interrogation by the CRISPR RNA-guided endonuclease Cas9. *Nature* 507 (7490):62-67. doi:10.1038/nature13011

Pubmed: [Author and Title](#)

CrossRef: [Author and Title](#)

Google Scholar: [Author Only](#) [Title Only](#) [Author and Title](#)

Trippens J, Greiner A, Schellwat J, Neukam M, Rottmann T, Lu YH, Kateriya S, Hegemann P, Kreimer G (2012) Phototropin Influence on Eyespot Development and Regulation of Phototactic Behavior in Chlamydomonas reinhardtii. *Plant Cell* 24 (11):4687-4702. doi:10.1105/tpc.112.103523

Pubmed: [Author and Title](#)

CrossRef: [Author and Title](#)

Google Scholar: [Author Only](#) [Title Only](#) [Author and Title](#)

Uhl R, Hegemann P (1990) Probing Visual Transduction in a Plant-Cell - Optical-Recording of Rhodopsin-Induced Structural-Changes from Chlamydomonas-Reinhardtii. *Biophys J* 58 (5):1295-1302

Pubmed: [Author and Title](#)

CrossRef: [Author and Title](#)

Google Scholar: [Author Only](#) [Title Only](#) [Author and Title](#)

Umen JG, Goodenough UW (2001) Control of cell division by a retinoblastoma protein homolog in Chlamydomonas. *Genes Dev* 15 (13):1652-1661. doi:10.1101/gad.892101

Pubmed: [Author and Title](#)

CrossRef: [Author and Title](#)

Google Scholar: [Author Only](#) [Title Only](#) [Author and Title](#)

Yamano T, Iguchi H, Fukuzawa H (2013) Rapid transformation of Chlamydomonas reinhardtii without cell-wall removal. *J Biosci Bioeng* 115 (6):691-694. doi:10.1016/j.jbiosc.2012.12.020

Pubmed: [Author and Title](#)

CrossRef: [Author and Title](#)

Google Scholar: [Author Only](#) [Title Only](#) [Author and Title](#)

Zheng X, Yang S, Zhang D, Zhong Z, Tang X, Deng K, Zhou J, Qi Y, Zhang Y (2016) Effective screen of CRISPR/Cas9-induced mutants in

rice by single-strand conformation polymorphism. *Plant Cell Rep* 35 (7):1545-1554. doi:10.1007/s00299-016-1967-1

Pubmed: [Author and Title](#)

CrossRef: [Author and Title](#)

Google Scholar: [Author Only](#) [Title Only](#) [Author and Title](#)

Zhu C, Bortesi L, Baysal C, Twyman RM, Fischer R, Capell T, Schillberg S, Christou P (2017) Characteristics of Genome Editing Mutations in Cereal Crops. *Trends Plant Sci* 22 (1):38-52. doi:10.1016/j.tplants.2016.08.009

Pubmed: [Author and Title](#)

CrossRef: [Author and Title](#)

Google Scholar: [Author Only](#) [Title Only](#) [Author and Title](#)

Zorin B, Hegemann P, Sizova I (2005) Nuclear-gene targeting by using single-stranded DNA avoids illegitimate DNA integration in *Chlamydomonas reinhardtii*. *Eukaryotic cell* 4 (7):1264-1272. doi:10.1128/EC.4.7.1264-1272.2005

Pubmed: [Author and Title](#)

CrossRef: [Author and Title](#)

Google Scholar: [Author Only](#) [Title Only](#) [Author and Title](#)

Zorin B, Lu Y, Sizova I, Hegemann P (2009) Nuclear gene targeting in *Chlamydomonas* as exemplified by disruption of the PHOT gene. *Gene* 432 (1-2):91-96. doi:10.1016/j.gene.2008.11.028

Pubmed: [Author and Title](#)

CrossRef: [Author and Title](#)

Google Scholar: [Author Only](#) [Title Only](#) [Author and Title](#)

Zou Y, Wenzel S, Muller N, Prager K, Jung EM, Kothe E, Kottke T, Mittag M (2017) An Animal-Like Cryptochrome Controls the *Chlamydomonas* Sexual Cycle. *Plant physiology* 174 (3):1334-1347. doi:10.1104/pp.17.00493

Pubmed: [Author and Title](#)

CrossRef: [Author and Title](#)

Google Scholar: [Author Only](#) [Title Only](#) [Author and Title](#)

Targeting of Photoreceptor Genes in *Chlamydomonas reinhardtii* via Zinc-finger Nucleases and CRISPR/Cas9

Andre Greiner, Simon Kelterborn, Heide Evers, Georg Kreimer, Irina Sizova and Peter Hegemann
Plant Cell; originally published online October 4, 2017;
DOI 10.1105/tpc.17.00659

This information is current as of October 12, 2017

Supplemental Data	/content/suppl/2017/10/04/tpc.17.00659.DC1.html /content/suppl/2017/10/12/tpc.17.00659.DC2.html
Permissions	https://www.copyright.com/ccc/openurl.do?sid=pd_hw1532298X&issn=1532298X&WT.mc_id=pd_hw1532298X
eTOCs	Sign up for eTOCs at: http://www.plantcell.org/cgi/alerts/ctmain
CiteTrack Alerts	Sign up for CiteTrack Alerts at: http://www.plantcell.org/cgi/alerts/ctmain
Subscription Information	Subscription Information for <i>The Plant Cell</i> and <i>Plant Physiology</i> is available at: http://www.aspб.org/publications/subscriptions.cfm